

**FDM & FEM ANALYSIS OF A PAD THRUST  
BEARING FOR THERMAL EFFECT**

**DISSERTATION**

Submitted in Partial Fulfilment of the  
Requirement for Award of the Degree

**Of**

**MASTER OF TECHNOLOGY**

**In**

**MECHANICAL ENGINEERING**

**By**

**NISHANT KUMAR  
(11304566)**

Under the Guidance of  
**MR. VIJAY SHANKER**



**DEPARTMENT OF MECHANICAL ENGINEERING**

**LOVELY PROFESSIONAL UNIVERSITY**

**PHAGWARA - 144411**

**2015**



**Lovely Professional University Jalandhar, Punjab**

## **CERTIFICATE**

I hereby certify that the work which is being presented in the dissertation entitled “**FDM & FEM Analysis of Pad Thrust Bearing for Thermal Effect**” in the partial fulfilment of the requirement for the award of degree of **Master of Technology** and submitted in Department of Mechanical Engineering, Lovely Professional University, Punjab is an authentic record of my own work carried out during period of Dissertation under the supervision of **Mr. Vijay Shankar, Assistant Professor**, Department of Mechanical Engineering, Lovely Professional University, Punjab.

The matter presented in this Dissertation has not been submitted by me anywhere for the award of any other degree or to any other institute.

Date:

(Nishant Kumar)

This is to certify that the above statement made by the candidate is correct to the best of my knowledge.

Date:

(Mr. Vijay Shanker)

Supervisor

---

The M-tech Dissertation Examination of Nishant Kumar, has been held on .....

Signature Of Examiner

## **ACKNOWLEDGEMENT**

No work is considered complete unless due indebtedness is expressed to all those, who made the work successful. Concentration, dedication, hard work & application are essential but not the only factors to achieve the desired goal. There must be supplemented by guidance, assistance and co-operation of people to make it a success. Every complete successful research paper is the result of many hands joined together.

Firstly I would like to thank Lovely Professional University who has given us this opportunity to do Dissertation in the field of Thermal Engineering.

I am thankful to my mentor Mr. Vijay Shankar and faculties of our university LPU who have directly or indirectly helped in this thesis.

I extremely like to thanks my friends and seniors who helped me, who encouraged me to do this.

It is warmth and efforts of my friends and well-wishers who have been a source of strength and confidence for me in the endeavour.

Finally, thanks to the Almighty who remained with me every time and always helped to direct me in the right direction which could lead me to my goal.

Nishant Kumar

## ABSTRACT

Hydrodynamic pad thrust bearings are widely used in high speed rotating machines such as pumps, compressors, turbines, turbo generators etc. because of their low friction, good load carrying capacity and high damping characteristics. Due to progress in technological trends, hydrodynamic pad thrust bearings are now being expected to be compact and work for elevated operating conditions i.e. at high loads and high speeds.

Hydrodynamic bearings rely on bearing motion to suck fluid into the bearing, and may have high friction and short life at speeds lower than design, or during starts and stops. An external pump or secondary bearing may be used for startup and shutdown to prevent damage to the hydrodynamic bearing. A secondary bearing may have high friction and short operating life, but good overall service life if bearing starts and stops are infrequent.

Thus, the objective of the present project is to carry out thermal analysis of the elasto- hydrodynamically lubricated pad thrust bearing by providing water cooling passages in the stationary thrust pad. It is pertinent to mention here that the prediction of accurate film thickness is essential for the correct estimation of the pressure distribution in bearing.

**Keywords:** Hydrodynamic pad thrust bearing, film thickness,

## CONTENTS

	Page no.
Abstract	IV
Contents	V
List of Figures	VI, VII
List of Tables	VIII
Nomenclature	IX, X
Chapter 1 Introduction	1
Chapter 2 Literature review	4
2.1 Isothermal analysis	
2.2 Thermal analysis	
2.3 Conclusions of literature review	
2.5 Scope of the study	
2.5 Objectives of present study	
Chapter 3 Governing equations and Problem Formulation	9
3.1 Reynolds equation	
3.2 Film thickness expression	
3.3 Elastic deformation of pad	
3.4 Energy equation	
3.5 FEM Modeling & Analysis	
3.6 FEM Simulation	
Chapter-4 Results & Discussion	28
Chapter-5 Conclusion and Future work	37
References	38

## **List of Figures**

<b>Figure</b>	<b>Description</b>
Fig. 1.1	Hydrodynamic thrust bearing
Fig.1.2	Pad profiles of hydrodynamic thrust bearing
Fig.3.1	Thrust Pad (sector shaped)
Fig3.2	Grid for a sector pad
Fig.3.3	Radial and angular velocities
Fig.3.4	Sector pad geometry
Fig.3.5	Sector shaped pad with passage for coolant
Fig.3.6	Pressure Distribution across the pad
Fig.3.7:	Sector pad showing heat balance
Fig 3.8	Ansys Model of Pad Thrust Bearing
Fig 3.9	Ansys Model of Pad
Fig 3.10	Ansys Meshed Model of Pad Thrust Bearing
Fig 3.11	Ansys Meshed Model of Pad
Fig.4.1	Plot of film thickness at a given radius but changing angular position
Fig.4.2	Plot of film thickness at a given angle but changing radial position
Fig.4.3	Film thickness at different nodal points
Fig.4.4	Plot of pressure at a given radius but with changing angular position
Fig.4.5	Plot of pressure at a given angle but with changing radial position
Fig.4.6	Pressure dome showing pressure at different nodal points of the pad
Fig.4.7	Pressure Contour
Fig.4.8	Temperature Contour
Fig.4.9	Radial Pressure Profile
Fig.4.10	Angular Pressure Profile

Fig.4.11

Validation Pressure Profile

## List of Tables

<b>Tables</b>	<b>Description</b>
Table 4.1:	INPUT DATA
Table 4.2:	FILM THICKNESS AT DIFFERENT NODAL POINTS
Table 4.3:	PRESSURE DISTRIBUTION AT DIFFERENT NODAL POINTS

## Nomenclature

- $a$  = minimum film thickness, m
- $b$  = amount of taper, m
- $h_1$  = inlet film thickness, m
- $h_L$  = outlet film thickness, m
- $h$  = film thickness at a radius  $r$ , m
- $h_f$  = convective heat transfer co-efficient of lubricant
- $H$  = non-dimensional thickness at a radius  $r$
- $K_h$  = thermal conductivity of oil
- $K_p$  = thermal conductivity of the pad
- $P$  = dimensionless pressure
- $p$  = hydrodynamic pressure, N/m<sup>2</sup>
- $R$  = coordinate in the radial direction, m
- $R_1$  = inner radius of the pad, m
- $R_2$  = outer radius, m
- $T$  = oil film temperature
- $T_p$  = pad temperature
- $t_p$  = pad thickness, m
- $T_{in}$  = oil film temperature
- $T_{atm}$  = atmospheric temperature
- $u_{1\theta}$  = particle velocity at  $z=h$ , m/s
- $u_{2\theta}$  = particle velocity at  $z=0$ , m/s
- $u$  = velocity component in tangential direction, m/s
- $u_r$  = velocity component in radial direction, m/s
- $u$  = velocity component in axial direction, m/s

$x$  = coordinate in X axis direction

$y$  = coordinate across the oil film, m

$z$  = coordinate along the axial direction, m

$\Theta$  = polar coordinate across the rotation of the runner, radians

$\beta$  = pad extent angle, radians

$\omega$  = angular velocity of runner and shaft, radians/s

$\rho$  = density of the lubricant at p, kg/m<sup>3</sup>

$\gamma$  = tilt about pitch line

$\Theta_p$  = angular extent of the pitch line of the pad, radians

$u_s, \eta$  = coefficient of viscosity at pressure p, Pa-s

## Chapter-1

### INTRODUCTION

---

Thrust bearing assembly includes structure of castellated and ring type configuration, where there is sandwich of ring like thrust washer and ring like dynamic race between the dynamic race and castellated end. Plurality of notches as well as Plurality of support region between the support regions are defined by castellated end configuration. On the top of the structure the thrust washer sits on the support structure. Intermittent support as well as intermittent un-support to the washer is been provided by the castellated end of the support structure.

The thrust washer initially flexes elastically at the unsupported regions and make hydrodynamic fluid wedge at the mating surface when a thrust load is been applied.

There are mainly two drawbacks of the hydrodynamic thrust bearing and they are wear and excessive friction. In many of the bearing such as roller or ball type of bearing have some limitation and constraints with respect to the price or cost, load capacity, durability as well as tolerance capability.

Because of the effect of contact deformation hydrodynamic bearings are underestimated at many places. Under the influence of load the shape of bearing changes. From a fixed position it's been rapidly used for positioning the member having dynamic motion and a fixed base. Moving member have a rigid flat face confronting towards the position having fixed base.

Structure of hydrodynamic thrust bearing posses:-

- Faces of the moving member are plated by plastic's thin film.
- Thin metal disk posses a center and on the both side of surface it's been called disk.
- Disk area is expanded radially outward from the center and are symmetrical through the whole surface of the disk.
- Between the fixed base and moving member flat face, disk is been positioned undulated where disk is in contact with planer surface face and flat rigid face with the base which is been fixed.
- After applying lubricant disk produce very thin film between the disk's undulations and rigid flat face of moving member which is cooperating.

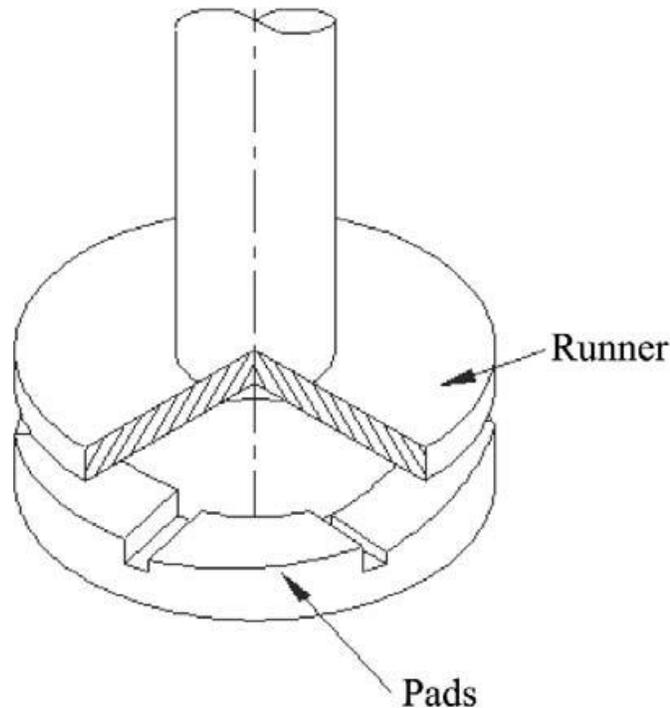


Fig 1.1 Hydrodynamic thrust bearing

Hydrodynamic pad thrust bearings are widely used in high speed rotating machines such as pumps, compressors, turbines, turbo generators etc. because of their low friction, good load carrying capacity and high damping characteristics. Due to progress in technological trends, hydrodynamic pad thrust bearings are now being expected to be compact and work for elevated operating conditions i.e. at high loads and high speeds.

Operating conditions of bearing produce huge viscous heat dissipation in lubrication film. About 60 to 70 % of the generated heat is carried away by lubricant itself through convection mode. However, remaining heat (30 to 40 %) goes in stationary pad through conduction mode. Thus, temperature of pad rises significantly. Being in direct contact of lubricant, heated pad reduces the viscosity of the lubricating oil significantly resulting in thinning of the oil. This causes drastic reduction in film thickness between the mating solids (pad and runner). Such situation may lead to metallic contacts.

An external pump or secondary bearing may be used for startup and shutdown to prevent damage to the hydrodynamic bearing. A secondary bearing may have high friction and short operating life, but good overall service life if bearing starts and stops are infrequent.

Fixed pad thrust bearings are available in literature having different pad shapes. Figures 1.2 (a) to 1.2 (d) illustrate the configuration of surface profiles on pads in thrust bearings.

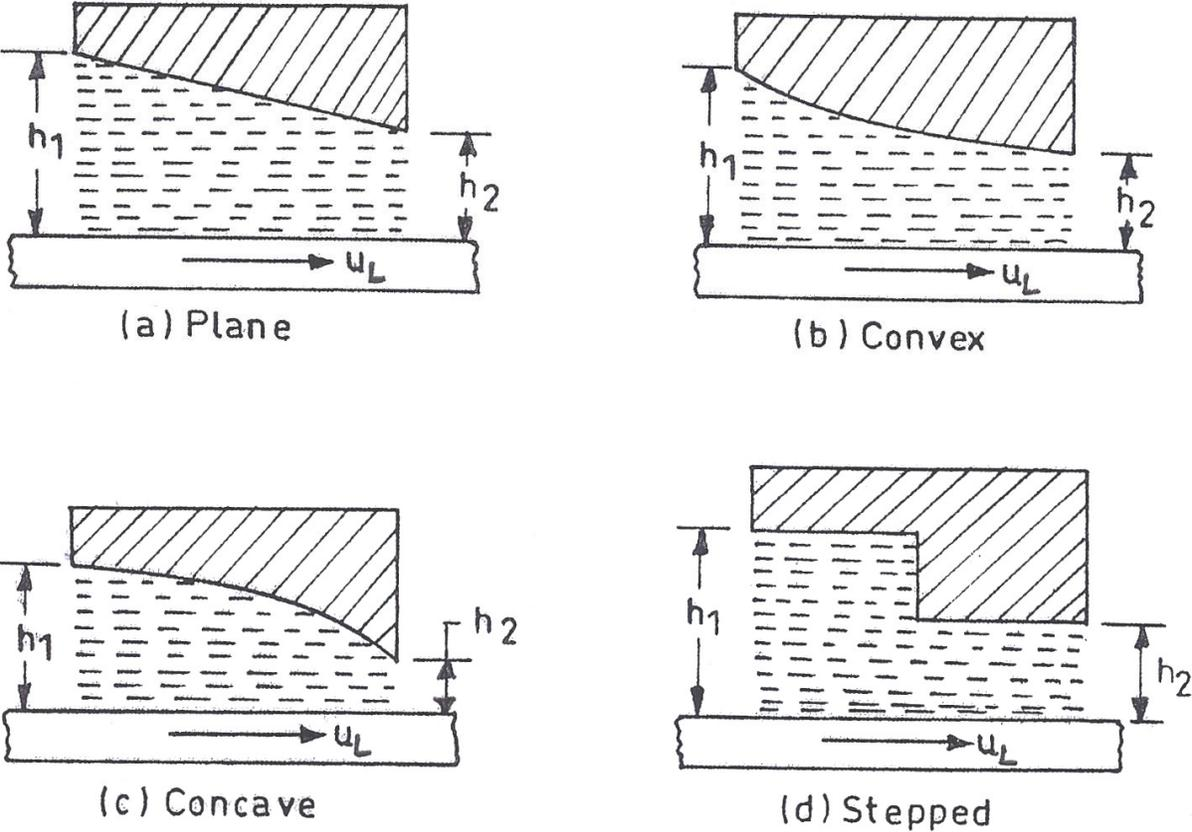


Fig 1.2 Pad profile of Hydrodynamic thrust bearing

## Chapter-2

### Literature Review

---

In this chapter, literature review have been incorporated briefly on the hydrodynamic pad thrust bearing. Available literature is grouped under “Thermal Analysis” and “Isotheraml Analysis” as follows:-

#### **2.1 Thermal Analysis :-**

Martin et al (2002) have studied together the principle of adjustable hydrodynamic bearing as well as their theoretical performance. In his paper he has explained the Reynolds equation considering non uniform fluid film thickness. In it he has also focus on advantages and characteristics benefits of hydrodynamic bearing.

Michal et al (2007) have investigated the performance of fluid film by investigating the temperature at the inlet. In his design he has proposed two lubricating methods for pad thrust bearing. First is bath lubrication and other one is direct lubrication. In lubrication process he has found that large load carrying capacity is only possible when the lubricant viscosity is high enough in direct lubrication. Because of high viscosity there will be thicker film which will reduce the temperature and on the effect of it deformation of the pad surface is decrease and pressure profile improve and finally load carrying capacity increase.

Q Zhu et al (2003) has studied the non linear response of hydrodynamic thrust bearing having sector shape in turbo- expander where the immediate load is applied. In his paper he has studied vibration equation for the axial shaft and time dependent Reynolds equation for oil film thickness. He then solve the time dependent Reynolds equation by applying FDM method and vibration equation by 4<sup>th</sup> order Runge- kutta method.

He has found the following results in his analysis:-

- On the transient response two parameters have significant effect and they are thickness of the film and the angle of inclination.
- For different film thickness and angle of inclination external excitation are non linear.

Samuel Cupillard et al (2008) has analyzed about slider bearing to keep the mechanism in condition state and find the optimum load carrying capacity. His study is been mainly focused on surface texture of slider bearing upon which the pressure build up and load carrying capacity depends. He experimented it for isothermal flow and for laminar and steady case. He found that energy is been converted into pressure where it was initially having converging contact. There is also losses in the second counter part. He lastly finalize that for getting more pressure gradient converging ratio should be more.

He has found the following results after the analysis:-

- Velocity profile is been dependent on the wall shape and it also finalize the pressure build up and pressure gradient by using continuity equation.
- When the process of recirculation occurs the value of pressure gradient decreases.
- Losses is minimum at the inlet in comparison to the outlet when the energy is been gained by the moving wall

M.Fowell et al (2007) introduced a new mechanism in the hydrodynamic lubrication called “inlet suction”. He told that it’s been only applicable for low convergence. In his research he has found that when the bearing surface slides on the surface its generate a lower pressure which is called subambient pressure which is comparatively less than the outer pressure or called the atmospheric pressure. Due to sub-ambient pressure the lubricant is been sucked between the surface. In this paper author has main focused in calculation of friction and supported load. In his analysis he found that inlet suction play a vital role in load support and friction reducing. This study is totally based on the principle of pressure drop due to which the lubricant is been sucked between the mating surface. He also show that after increasing the flow of lubricant the pressure which is generated can be enhanced and the load support increases and friction also reduces.

Wang et al (2004) has analyzed spring supported thrust bearing by applying finite difference method. Wang has generalised thermo-elastic deformation equation, Reynolds equation and energy equation by applying finite difference method. During his research he analysed many characterial mechanism which leave their impact on bearing during hydrodynamic lubrication theory. And he found that many of the factors such as pad geometry and its inclination as well as the thickness of the film effect the performance of bearing.

T.Jintanawan et al (2004) has analysed, after having significant effect on some of the parameters the nature of the bearing changes. When stiffness increases axial vibration reduces and similarly increase in damping make the system unbalanced. The hub vibration has no motion in direct transmission from disk to base.

Glavatskih et al (2005) investigated the effect on power loss, thickness of the film and the operational temperature by the surface texturing. For it he has taken a large diameter bearing whose textured surface has depth of 10 micrometers and when lubricant is been supplied at constant flow rate there is been significant effect on power loss and thickness of film.

Tonasz woloszynski et al (2013) have taken four methods of discretisation such as finite difference method, finite element method, finite volume method and spectral element method for knowing pressure function and for knowing the height of film, load carrying capacity and coefficient of friction different integration method is been considered. He has taken different geometries of textured surface and calculated the pressure function, coefficient of friction and load carrying capacity and found that spectral element method and gauss quadrature method shows the accurate result that fits the bearing geometry.

## **2.2 Isotheraml Analysis:-**

Ashour at al (2005) focused on calculating the elastic distortion of the pad of the pad thrust bearing by solving elasticity equation and Reynolds equation. He has tried a new approach where he was loading in stepwise format so that he could reach to load which he has targeted. They compared their results in both the cases of lubrication flow which is along the direction of flow and across the direction of flow where the thickness of film changes and they have validated their results.

Khonsari and Booser (2006) researched in basically three areas :- experimental evaluations and operating experience relating to contaminant detrimental effects to the particle size and hardness; importance of film thickness; and self propagating damage with high chromium steel rotors and chlorine oil additives. From avoiding damaging of flush temperature scuffing failure they have propose a fix particle size limit.

Hashimoto (2006) has theoretically and experimentally investigated an influence of lubrication conditions on the performance characteristics of sector shaped pad thrust bearings, which were subjected to the effects of both turbulence and fluid film inertia.

Bryant et al. (2004) have developed a lumped parameter model for hydrodynamically lubricated bearings: elements that feature fully lubricated contact between surfaces in relative motion. The bearing models have been represented as bond graphs. These lumped parameter models were synthesised from solutions of the Reynolds equation for various bearing geometries, and include normal motion and squeeze film effects

Tala-Ighil et al (2007) have investigated the influence of textured surface on pad thrust bearing when the operating condition were under the influence of steady state. In their work they have quantify the evolution of the textured surface parameters characteristics and deduced their optimized value and enhance the performance of bearing by considering optimized value

### **2.3 Conclusions of literature review:-**

Based on the literature review mentioned above, the following points have been noted:-

- Influence of surface texturing on hydrodynamic lubrication of fixed pad thrust bearings in terms of bearing power loss, operating temperature, and oil film thickness
- The performance of the pad bearing by progressively taking into account the optimized values of texture parameters, especially the textures disposition.
- Investigated the influence of pad active surface geometry on main characteristics such as temperature profile, film thickness and pressure field.
- Effect of oil viscosity on the performance of fixed pad thrust bearings in a wide range of shaft speeds and specific bearing loads.
- Dealing with the cooling passages in the stationary pad for controlling the temperature at the contact conjunction.

### **2.4 Scope of the study:-**

- While computing the film thickness there will be two cases of consideration
  - Without Pad deformation
  - With Pad deformation

- Thermal conductivity of the pad can be assumed independent of temperature, as well as dependent of temperature.
- The position of maximum pressure developed along the direction of flow due to the hydrodynamic action.

## 2.5 Objectives of the study:-

The objective of this project is to carry out thermal analysis of the hydrodynamically lubricated pad thrust bearing functioning at elevated operating conditions by providing water cooling passages in the stationary thrust pad. Various designs of water passages will be conceived for the implementation and accordingly elastic deformation in pad will be computed for the estimation of correct values of film thickness.

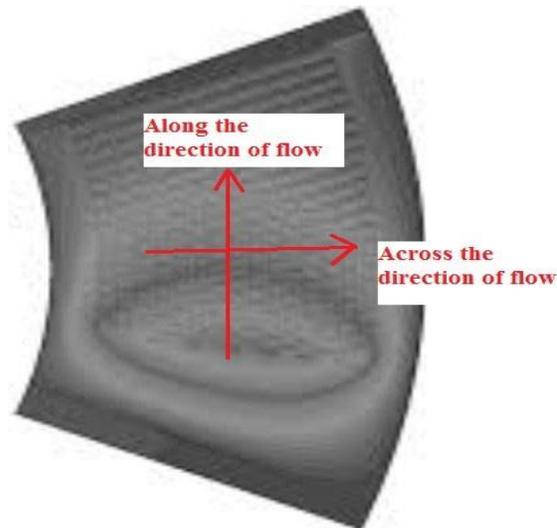


Fig-2.1

## Chapter-3

### Governing Equations and Problem Formulation

---

In this section, a brief discussion of the related governing equation and mathematical formulation of the problems. Due to sector shape the governing equation is in cylindrical polar coordinates:-

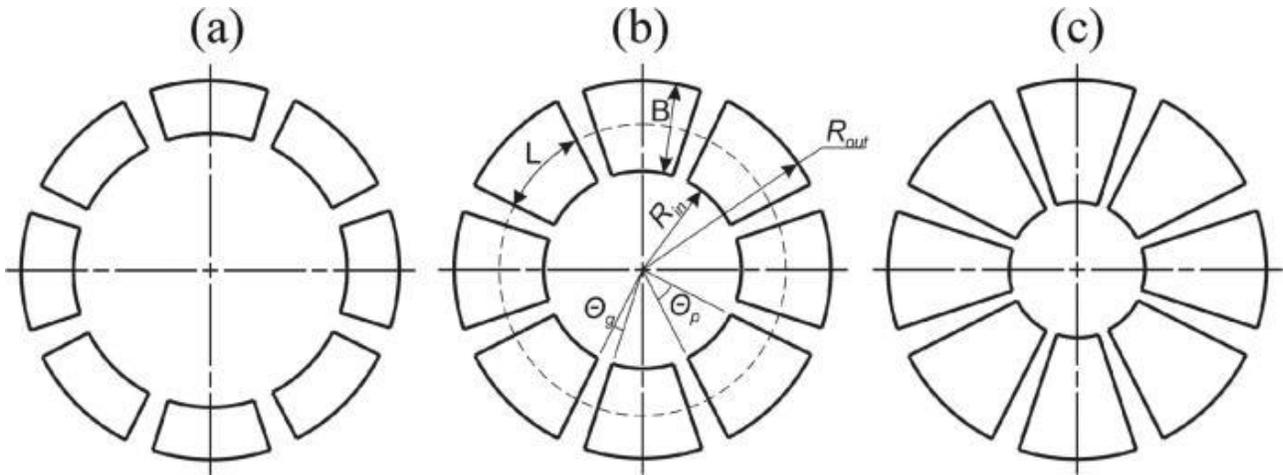


Fig 3.1 Thrust Pad (Sector Shaped)

#### Method:-

In the entire section of study the prime focus is the pressure exerted by the lubricant on the pad of the pad thrust bearing. For studying the behavior and the thickness of the lubricant on the surface of the plate the best fit is Reynold equation through which we can analyse the lubricant behavior which passes between the runner and the pad. Reynolds equation helps me to find out the pressure distribution on the entire surface. So in my thesis ore research I have decided to solve the Reynold equation which is a partial differential equation under the proper defined condition.

In this study three consideration have been mainly included and they are:

- Thermal effect
- Pressure distribution on entire surface
- Elastic deformation

Here is the flow chart of numerically solving the thrust bearing problem:-

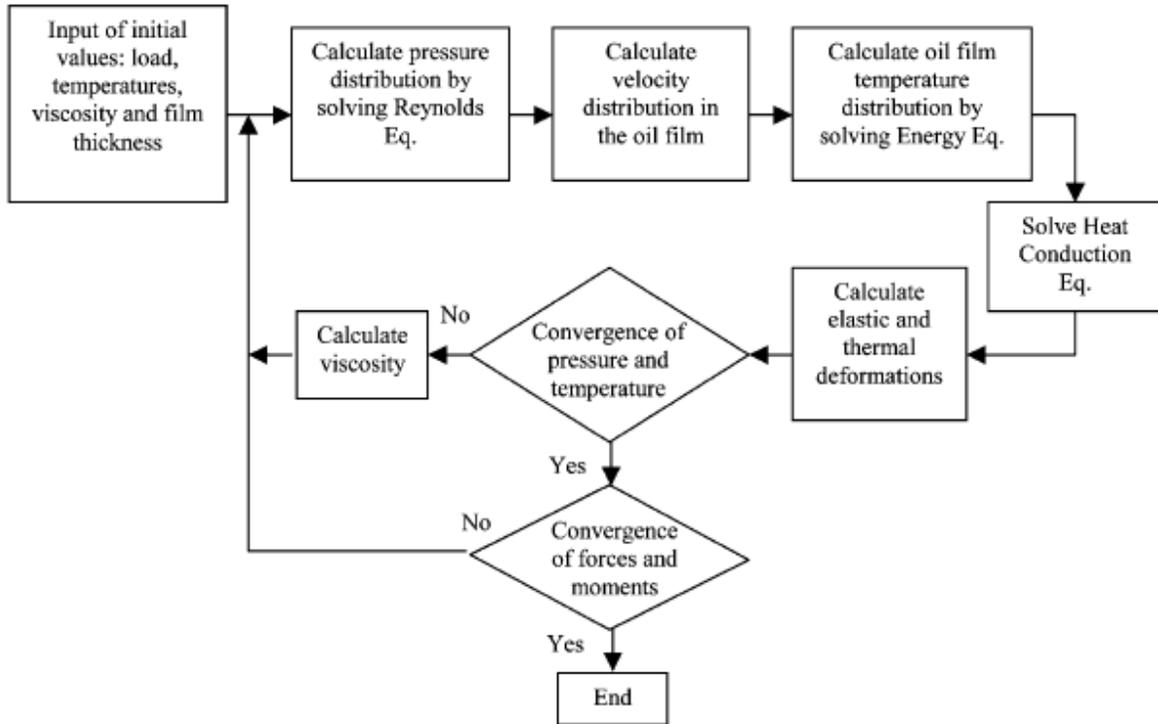


Fig 3.2 Procedure Flow Chart

**Film thickness equation** (cylindrical polar coordinates):

For sector pad geometry, under isothermal condition the film thickness is a function of both circumferential and radial coordinates.

The compact film thickness expression reported by Etsion considers variation in tangential and radial directions both and is given by:

$$h = h_p + \gamma r \sin(\theta_p - \theta) \quad (3.1)$$

The non-dimensional form of thickness given by Eq. (3.1) can be written by using

$$H = h/h_p, R = r/R_2, \varepsilon = \gamma R_2 / h_p$$

$$H = 1 + \varepsilon R \sin(\theta_p - \theta) \quad (3.2)$$

**Reynolds equation** (cylindrical polar coordinates)

$$\frac{1}{r} \frac{\partial}{\partial r} \left( r h^3 \frac{\partial P}{\partial r} \right) + \frac{1}{r^2} \frac{\partial}{\partial \theta} \left( h^3 \frac{\partial P}{\partial \theta} \right) = 6\eta r \omega \frac{\partial h}{\partial \theta} \quad (3.3)$$

**Finite Difference Formulation of Reynolds equation:-**

To non-dimensionalise the Reynolds equation, the above equation can be non-dimensionalised by using the following relations:

$$R = \frac{r}{R_2}, H = \frac{h}{b}, P = \frac{pb^2}{\eta NL^2}, \omega = \frac{2\pi N}{60}$$

where,

$R_2$ = outer radius of the sector pad,

$h$ =film thickness,

$b$ =amount of taper,

$p$ =pressure,

$\eta$ =viscosity of lubricant,

$\omega$ =angular velocity

**L.H.S.**

$$\begin{aligned} &= \frac{1}{r} \frac{\partial}{\partial r} \left( r h^3 \frac{\partial P}{\partial r} \right) + \frac{1}{r^2} \frac{\partial}{\partial \theta} \left( h^3 \frac{\partial P}{\partial \theta} \right) \\ &= \frac{1}{R_2} \frac{\partial}{\partial R} \left( R R_2 H^3 b^3 \frac{\eta NL^2}{b^2} \frac{\partial P}{R_2 \partial R} \right) + \frac{1}{R R_2} \frac{\partial}{\partial \theta} \left( H^3 b^3 \frac{\eta NL^2}{b^2} \frac{\partial P}{\partial \theta} \right) \\ &= \frac{6\eta NL^2}{R^2} \left[ \frac{\partial}{\partial R} \left( R H^3 \frac{\partial P}{\partial R} \right) + \frac{1}{R} \frac{\partial}{\partial \theta} \left( H^3 \frac{\partial P}{\partial \theta} \right) \right] \end{aligned}$$

**R.H.S**

$$\begin{aligned} &= 6\eta r \omega \frac{\partial h}{\partial \theta} = 6\eta R R_2 \omega b \frac{\partial H}{\partial \theta} \\ &= 12\eta \pi N R R_2 \frac{\partial H}{\partial \theta} \end{aligned}$$

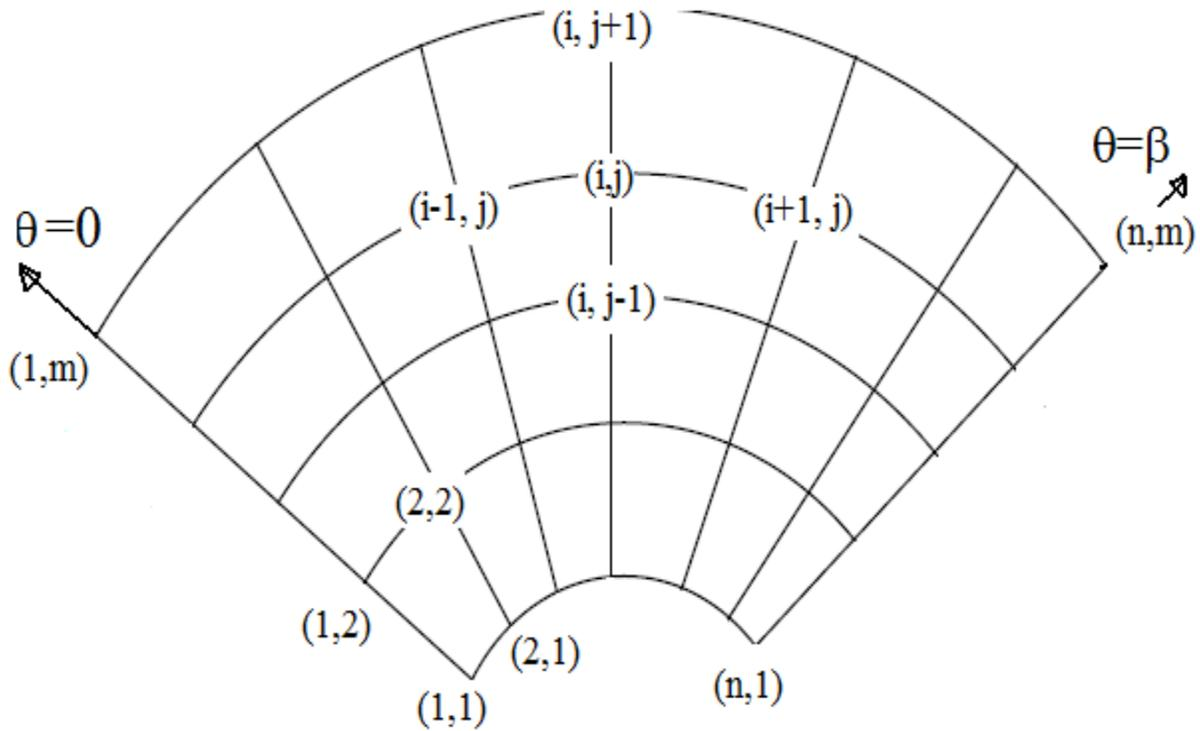
Now,

$$\frac{6\eta NL^2}{R^2} \left[ \frac{\partial}{\partial R} \left( RH^3 \frac{\partial P}{\partial R} \right) + \frac{1}{R} \frac{\partial}{\partial \theta} \left( H^3 \frac{\partial P}{\partial \theta} \right) \right] = 12\eta\pi NRR_2 \frac{\partial H}{\partial \theta}$$

$$\left[ \frac{\partial}{\partial R} \left( RH^3 \frac{\partial P}{\partial R} \right) + \frac{1}{R} \frac{\partial}{\partial \theta} \left( H^3 \frac{\partial P}{\partial \theta} \right) \right] = 12\pi R \left( \frac{R_2}{L} \right)^2 \frac{\partial H}{\partial \theta}$$

To discretize the non-dimensional form of the Reynolds equation:-

The non-dimensional form of Reynolds equation can be put into finite difference form by using central difference technique for each of the terms in the equation.



Grid for a sector pad

Fig 3.2

We can write the non-dimensionalised Reynolds equation in the following form:-

$$\frac{\partial RH^3}{\partial R} \left( \frac{\partial P}{\partial R} \right) + RH^3 \frac{\partial^2 P}{\partial R^2} + \frac{1}{R} \left( \frac{\partial H^3}{\partial \theta} \right) + \frac{H^3}{R} \frac{\partial^2 P}{\partial \theta^2} = 12\pi R \left( \frac{R_2}{L} \right)^2 \frac{\partial H}{\partial \theta}$$

Using central differentiation each term can be written as:

$$\begin{aligned} \frac{\partial RH^3}{\partial R} &= \frac{(RH^3)_{i,j+1} - (RH^3)_{i,j-1}}{2(\Delta R)}, & \frac{\partial P}{\partial R} &= \frac{P_{i,j+1} - P_{i,j-1}}{2(\Delta R)} \\ \frac{\partial^2 P}{\partial R^2} &= \frac{P_{i,j+1} - 2P_{i,j} + P_{i,j-1}}{(\Delta R)^2}, & \frac{\partial H^3}{\partial \theta} &= \frac{H^3_{i+1,j} - H^3_{i-1,j}}{2(\Delta \theta)} \\ \frac{\partial^2 P}{\partial \theta^2} &= \frac{P_{i+1,j} - 2P_{i,j} + P_{i-1,j}}{(\Delta \theta)^2}, & \frac{\partial H}{\partial \theta} &= \frac{H_{i+1,j} - H_{i-1,j}}{2(\Delta \theta)} \\ \frac{\partial P}{\partial \theta} &= \frac{P_{i+1,j} - P_{i-1,j}}{2(\Delta \theta)} \end{aligned}$$

Substituting these in equation (4) we have:

$$\begin{aligned} &= \left[ \frac{(RH^3)_{i,j+1} - (RH^3)_{i,j-1}}{2(\Delta R)} \right] \left[ \frac{P_{i,j+1} - P_{i,j-1}}{2(\Delta R)} \right] (RH^3)_{i,j} \left[ \frac{P_{i,j+1} - 2P_{i,j} + P_{i,j-1}}{(\Delta R)^2} \right] \\ &+ \frac{1}{R_{i,j}} \left[ \frac{H^3_{i+1,j} - H^3_{i-1,j}}{2(\Delta \theta)} \right] \left[ \frac{P_{i+1,j} - P_{i-1,j}}{2(\Delta \theta)} \right] \\ &+ \frac{H^3_{i,j}}{R_{i,j}} \left[ \frac{P_{i+1,j} - 2P_{i,j} + P_{i-1,j}}{(\Delta \theta)^2} \right] = 12\pi R_{i,j} \left( \frac{R_2}{L} \right)^2 \left[ \frac{H_{i+1,j} - H_{i-1,j}}{2(\Delta \theta)} \right] \end{aligned}$$

Or,

$$\begin{aligned} &\left[ \frac{(RH^3)_{i,j+1} - (RH^3)_{i,j-1}}{2(\Delta R)} \right] \left[ \frac{P_{i,j+1} - P_{i,j-1}}{2(\Delta R)} \right] (RH^3)_{i,j} \left[ \frac{P_{i,j+1} - 2P_{i,j} + P_{i,j-1}}{(\Delta R)^2} \right] \\ &+ \frac{1}{R_{i,j}} \left[ \frac{H^3_{i+1,j} - H^3_{i-1,j}}{2(\Delta \theta)} \right] \left[ \frac{P_{i+1,j} - P_{i-1,j}}{2(\Delta \theta)} \right] \\ &+ \frac{H^3_{i,j}}{R_{i,j}} \left[ \frac{P_{i+1,j} - 2P_{i,j} + P_{i-1,j}}{(\Delta \theta)^2} \right] - 12\pi R_{i,j} \left( \frac{R_2}{L} \right)^2 \left[ \frac{H_{i+1,j} - H_{i-1,j}}{2(\Delta \theta)} \right] \\ &= 2P_{i,j} \left[ \frac{(RH^3)_{i,j}}{(\Delta R)^2} + \frac{H^3_{i,j}}{R_{i,j}(\Delta \theta)} \right] \end{aligned}$$

Or,

$$\begin{aligned}
& \left[ \frac{(RH^3)_{i,j+1} - (RH^3)_{i,j-1}}{2(\Delta R)} \right] \left[ \frac{P_{i,j+1} - P_{i,j-1}}{2(\Delta R)} \right] (RH^3)_{i,j} \left[ \frac{P_{i,j+1} - 2P_{i,j} + P_{i,j-1}}{(\Delta R)^2} \right] \\
& + \frac{1}{R_{i,j}} \left[ \frac{H^3_{i+1,j} - H^3_{i-1,j}}{2(\Delta\theta)} \right] \left[ \frac{P_{i+1,j} - P_{i-1,j}}{2(\Delta\theta)} \right] \\
& + \frac{H^3_{i,j}}{R_{i,j}} \left[ \frac{P_{i+1,j} - 2P_{i,j} + P_{i-1,j}}{(\Delta\theta)^2} \right] - 12\pi R_{i,j} \left( \frac{R_2}{L} \right)^2 \left[ \frac{H_{i+1,j} - H_{i-1,j}}{2(\Delta\theta)} \right] \\
& = \frac{2H^3_{i,j}}{(\Delta R)^2(\Delta\theta)^2} \left[ R_{i,j}(\Delta\theta)^2 + \frac{(\Delta R)^2}{R_{i,j}} \right] P_{i,j}
\end{aligned}$$

Now, assuming:

$$AA1 = 2H^3_{i,j} \left[ R_{i,j}(\Delta\theta)^2 + \frac{(\Delta R)^2}{R_{i,j}} \right]$$

$$AA2 = (RH^3)_{i,j}$$

$$AA3 = \frac{(RH^3)_{i,j+1}}{4}$$

$$AA4 = \frac{(RH^3)_{i,j-1}}{4}$$

$$AA5 = \frac{H^3_{i,j}}{R_{i,j}}$$

$$AA6 = \frac{(H^3_{i+1,j} - H^3_{i-1,j})}{4R_{i,j}}$$

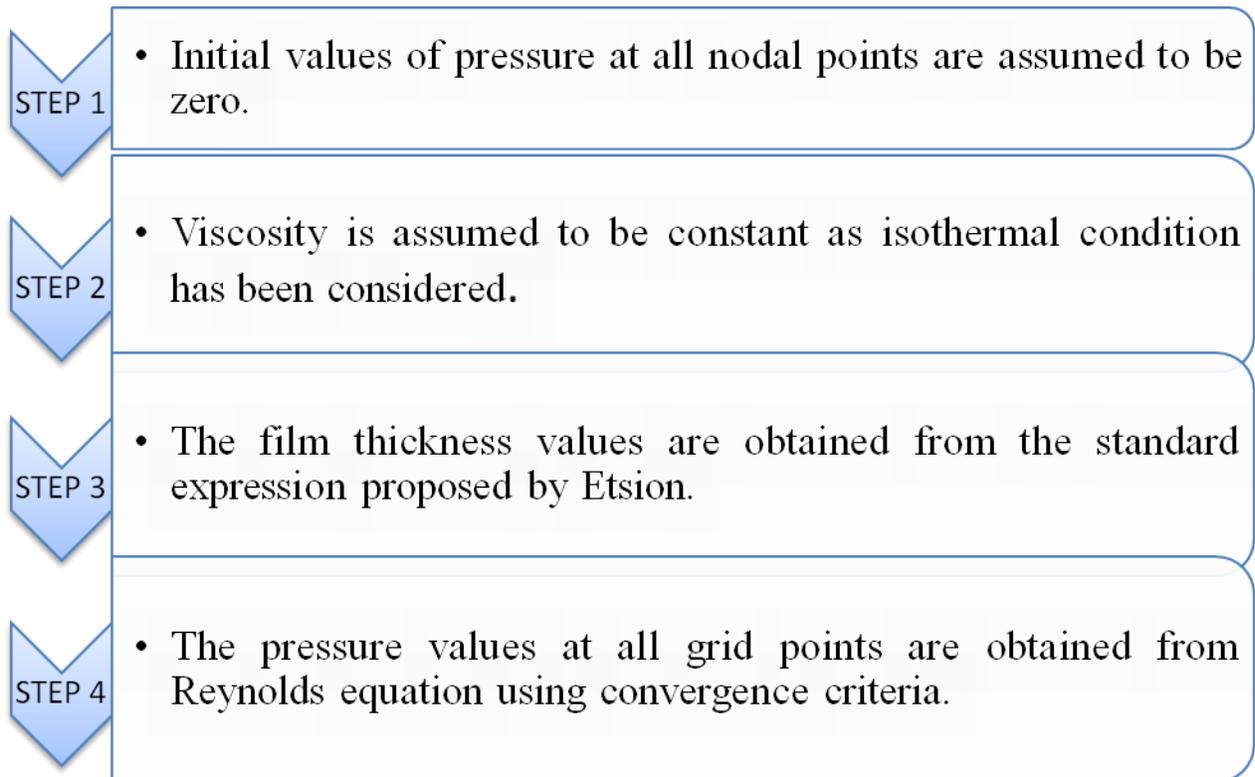
Or,

$$\begin{aligned}
P_{i,j} = & \frac{(\Delta R)^2 (\Delta \theta)^2}{AA1} \left[ \left( \frac{AA3 - AA4}{(\Delta R)^2} + \frac{AA2}{(\Delta R)^2} \right) P_{i,j+1} \right. \\
& + \left( \frac{AA2}{(\Delta R)^2} - \frac{AA3 - AA4}{(\Delta R)^2} \right) P_{i,j-1} + \frac{AA6}{(\Delta \theta)^2} (P_{i+1,j} - P_{i-1,j}) \\
& + \left. \frac{AA5}{(\Delta \theta)^2} (P_{i+1,j} - P_{i-1,j}) \right] \\
& + \frac{(\Delta R)^2 (\Delta \theta)^2}{AA1} 12\pi R_{i,j} \left( \frac{R_2}{L} \right)^2 \left[ \frac{H_{i-1,j} - H_{i+1,j}}{2(\Delta \theta)} \right]
\end{aligned}$$

$$\begin{aligned}
P_{i,j} = & \frac{1}{AA1} \left( (\Delta \theta)^2 (AA3 - AA4 + AA2) P_{i,j+1} \right. \\
& + (\Delta \theta)^2 (AA2 - AA3 + AA4) P_{i,j-1} + \Delta R^2 (AA5 + AA6) P_{i+1,j} \\
& + \Delta R^2 (AA5 - AA6) P_{i-1,j} \\
& \left. + \frac{(\Delta R)^2 (\Delta \theta)^2}{AA1} \left( 12\pi R_{i,j} \left( \frac{R_2}{L} \right)^2 (H_{i-1,j} - H_{i+1,j}) \right) \right)
\end{aligned}$$

$$\begin{aligned}
P_{i,j} = & \frac{(\Delta \theta)^2 (AA3 - AA4 + AA2)}{AA1} P_{i,j+1} + \frac{(\Delta \theta)^2 (AA2 - AA3 - AA4)}{AA1} P_{i,j-1} \\
& + \frac{\Delta R^2 (AA5 + AA6)}{AA1} P_{i+1,j} + \frac{\Delta R^2 (AA5 - AA6)}{AA1} P_{i-1,j} \\
& + 6\pi R_{i,j} \frac{(\Delta R)^2 (\Delta \theta)}{AA1} \left( \frac{R_2}{L} \right)^2 (H_{i-1,j} - H_{i+1,j})
\end{aligned}$$

### Flow Chart for calculation of pressure profile:-



### Convergence Criteria for Pressure:-

$$\sum_{i=1}^n \sum_{j=1}^m \frac{|P_{i,j}^{K+1} - P_{i,j}^K|}{P_{i,j}^{K+1}} < \varepsilon_p$$

where, K= no. of iteration

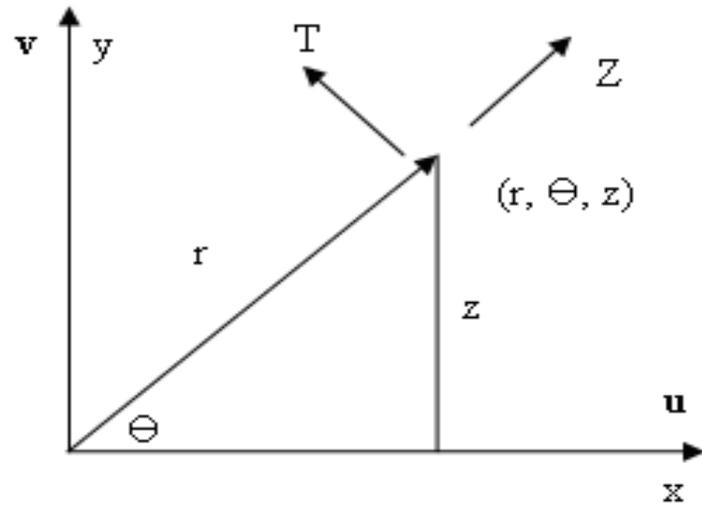


**Fig.3.3 Radial and angular velocities**

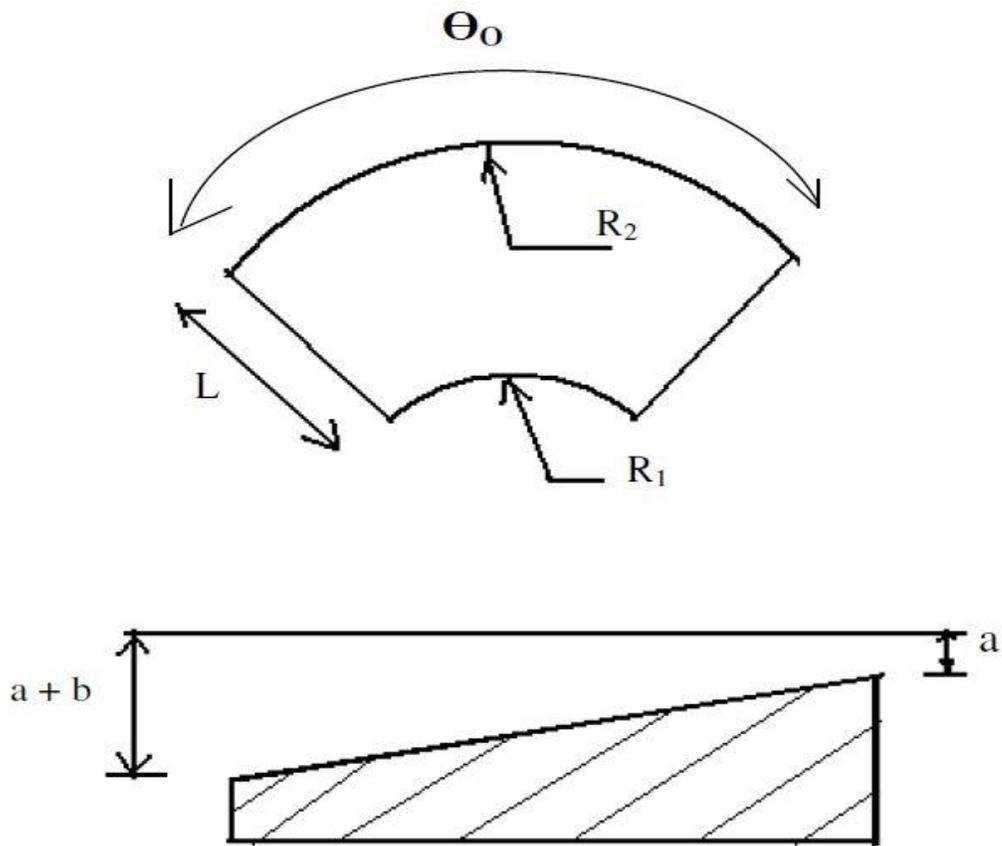


**Fig.3.4 Sector pad geometry**

**Elastic deformation of pad (biharmonic equation in polar form):**

$$\frac{\partial^4 Z}{\partial R^4} + \frac{2}{R} \left( \frac{\partial^3 Z}{\partial R^3} \right) - \frac{1}{R} \left( \frac{\partial^2 Z}{\partial R^2} \right) + \frac{1}{R^3} \frac{\partial Z}{\partial R} - \frac{2}{R^3} \frac{\partial^3 Z}{\partial R \partial \theta^2} + \frac{4}{R^4} \frac{\partial^2 Z}{\partial \theta^2} + \frac{2}{R^2} \frac{\partial^4 Z}{\partial R^2 \partial \theta^2} + \frac{1}{R^4} \frac{\partial^4 Z}{\partial \theta^4} + K_1 Z = P$$

Where

$$R = \frac{r}{r_0} \quad r_0 = \text{being outer radius,}$$

$$K_1 = \frac{K r_0^4}{D}$$

$$Z = \frac{z}{t}$$

$$P = \frac{p r_0^4}{D t}$$

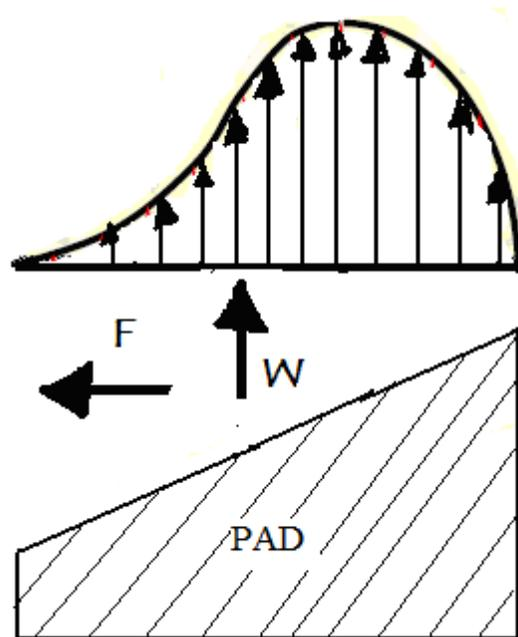


Fig.3.5 Pressure Distribution across the pad

## Thermal analysis

Besides the usual assumptions of lubrication theory, the following assumptions are made:

- The lubricating surfaces of the pad and the disk are rigid, and their thermal and elastic distortions are disregarded.
- The velocity gradient and heat conduction in the  $r$  and  $\theta$  directions can be ignored in comparison with those in the  $z$  direction.
- The specific heat at constant pressure  $C_p$  and the coefficient of thermal expansion  $\alpha$  of the lubricating oil are constant.
- The thermal conductivity of the lubricating oil  $K_o$  and the thermal conductivity of the pad  $K_s$  are constant.
- The coefficient of viscosity  $\mu$  and the density  $\rho$  of the lubricating oil are functions of temperature  $T$  only.

## Energy equation (Cylindrical polar coordinates):-

To consider the temperature rise in a fluid under shear, the balance of the heat produced by viscous dissipation, the heat flow by convection and conduction, and the heat accumulated in the fluid must be investigated. An equation that describes such a balance of energy is called the energy equation.

During the lubrication process energy is dissipated in two ways: through the action of viscous friction and through compression (smaller effect). Both of these sources liberate heat which changes the fluid temperature which in turn changes the viscosity of fluid which in turn changes the dissipation as well as flow and pressure.

$$K \left( \frac{\partial^2 T}{\partial r^2} + \frac{1}{r} \frac{\partial T}{\partial r} + \frac{1}{r^2} \frac{\partial^2 T}{\partial \theta^2} + \frac{\partial^2 T}{\partial z^2} \right) + \mu \left( \left( \frac{\partial u}{\partial z} \right)^2 + \left( \frac{\partial v}{\partial z} \right)^2 \right) \\ = \rho c_p \left( u \frac{\partial T}{\partial r} + \frac{v}{r} \frac{\partial T}{\partial \theta} + w \frac{\partial T}{\partial z} \right)$$

The heat conduction equation within the pad under steady state condition and assuming no heat generation is given by:-

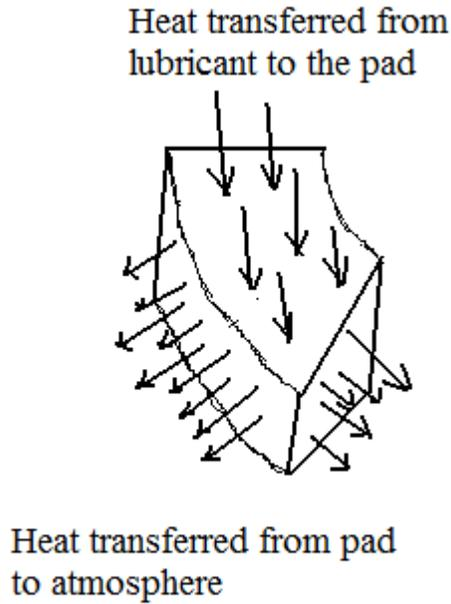


Fig 3.7

$$\frac{K_{\theta} \partial^2 T_B}{r^2 \partial \theta^2} + \frac{K_r \partial}{r \partial r} \left( r \frac{\partial T_B}{\partial r} \right) + K_z \frac{\partial^2 T_B}{\partial z^2} = 0$$

Or,

$$\frac{K_{\theta}}{r^2} \frac{\partial^2 T_B}{\partial \theta^2} + \frac{K_r}{r} \frac{\partial T_B}{\partial r} + K_r \frac{\partial^2 T_B}{\partial r^2} + K_z \frac{\partial^2 T_B}{\partial z^2} = 0$$

where,  $T_B$  = pad temperature,

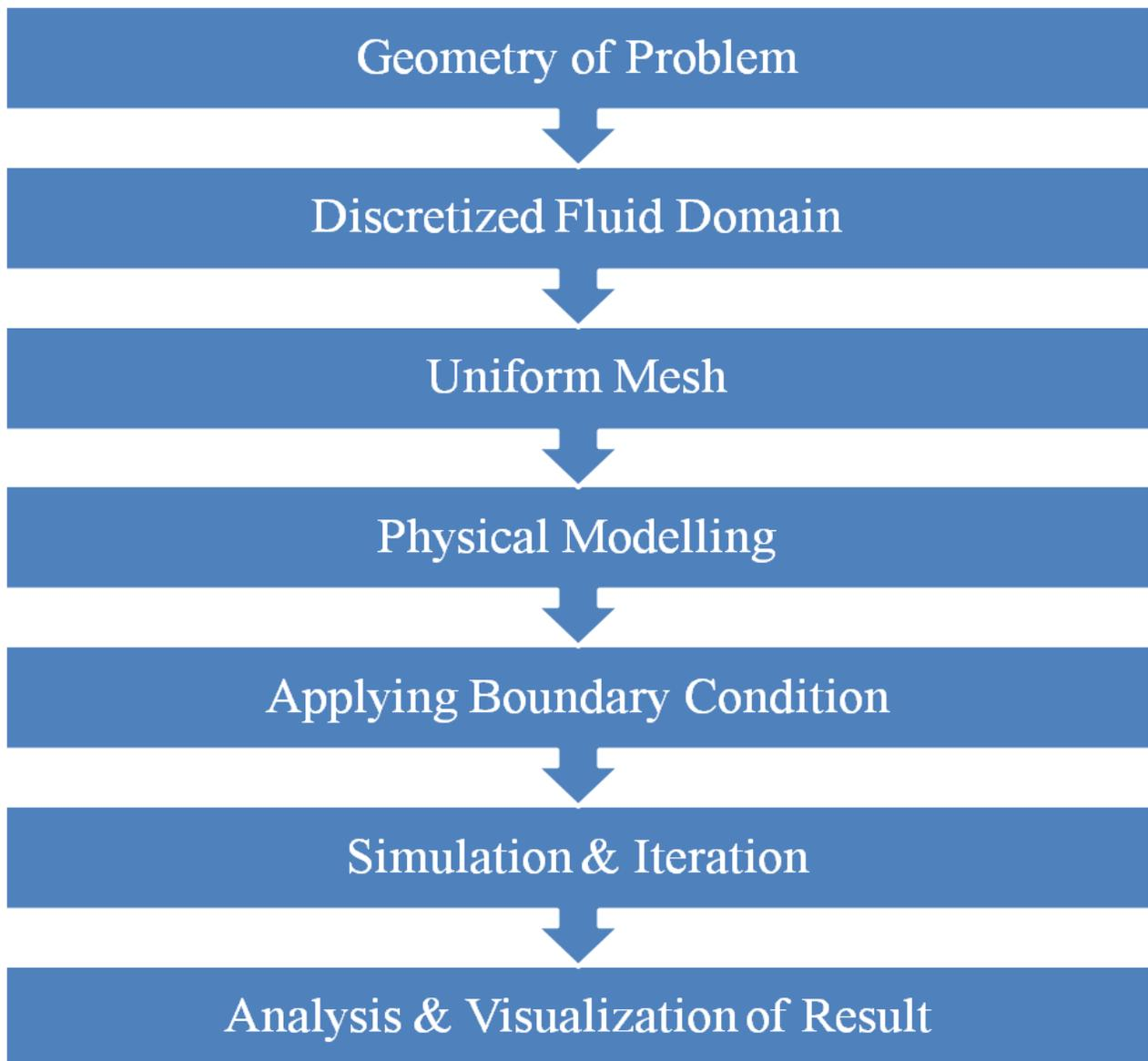
$K_{\theta}$ ,  $K_r$  &  $K_z$  = thermal conductivity of the pad material in circumferential, radial and z-directions respectively

## **FEM Modeling & Analysis:-**

In the field of Computer-aided Engineering ANSYS software is used to construct the model of the components or the system and there we can also apply operating loads and other design consideration.

With the help of this software we can also study the physical responses such as pressure distribution, Temperature distribution and the stress levels as well.

Basic procedures that been used in this analysis are :



## SIMULATION:-

ANSYS FLUENT 14.5 is used for making 3D geometry of the pad thrust bearing and then after meshing in fluent, the flow of the lubricant SAE-30 is been analyzed. In it UDF function which means user defined function is been used which is already loaded in FLUENT 14.5 solver to increase the features.

By using UDF we have defined our own boundary conditions and material properties as well as we have customize the parameters of the model and initialize the solution.

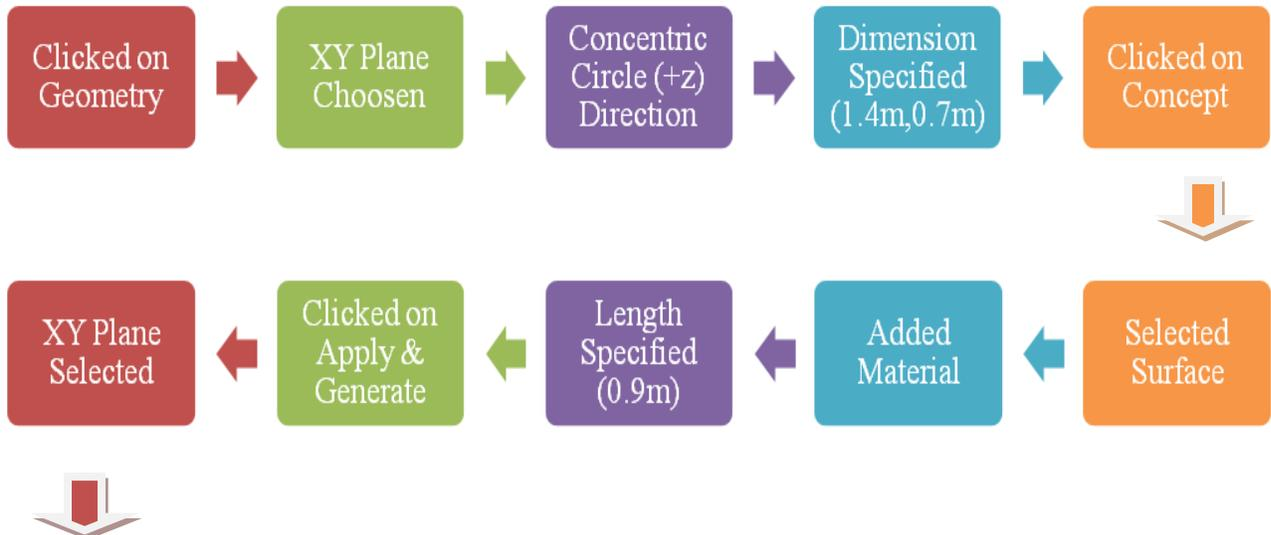
The analysis solution consist of seven major steps which are mentioned step by step as follows:-

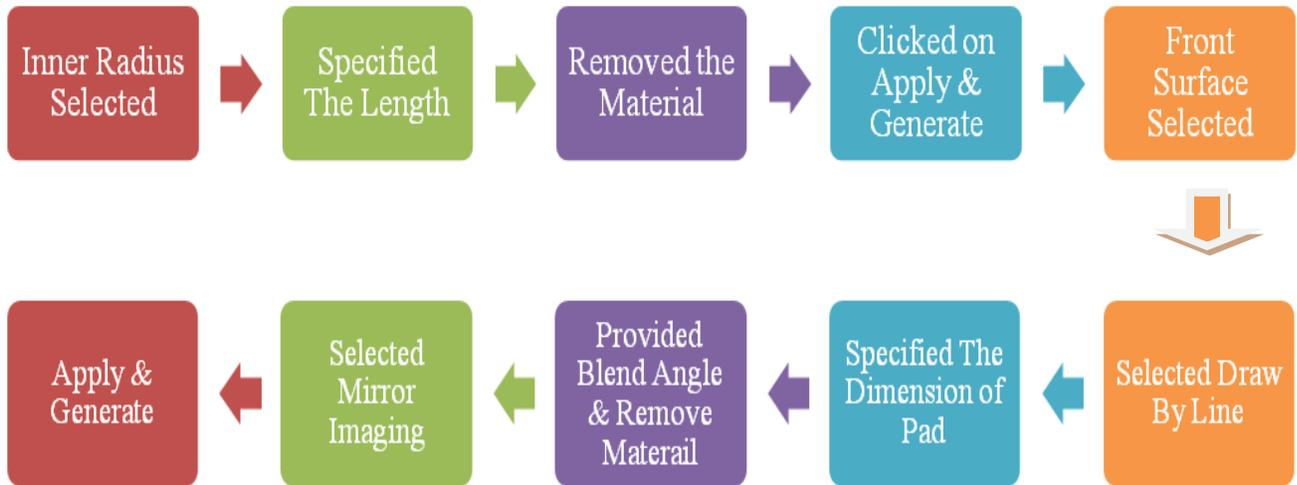
**STEP 1**→Start up & Pre analysis of problem



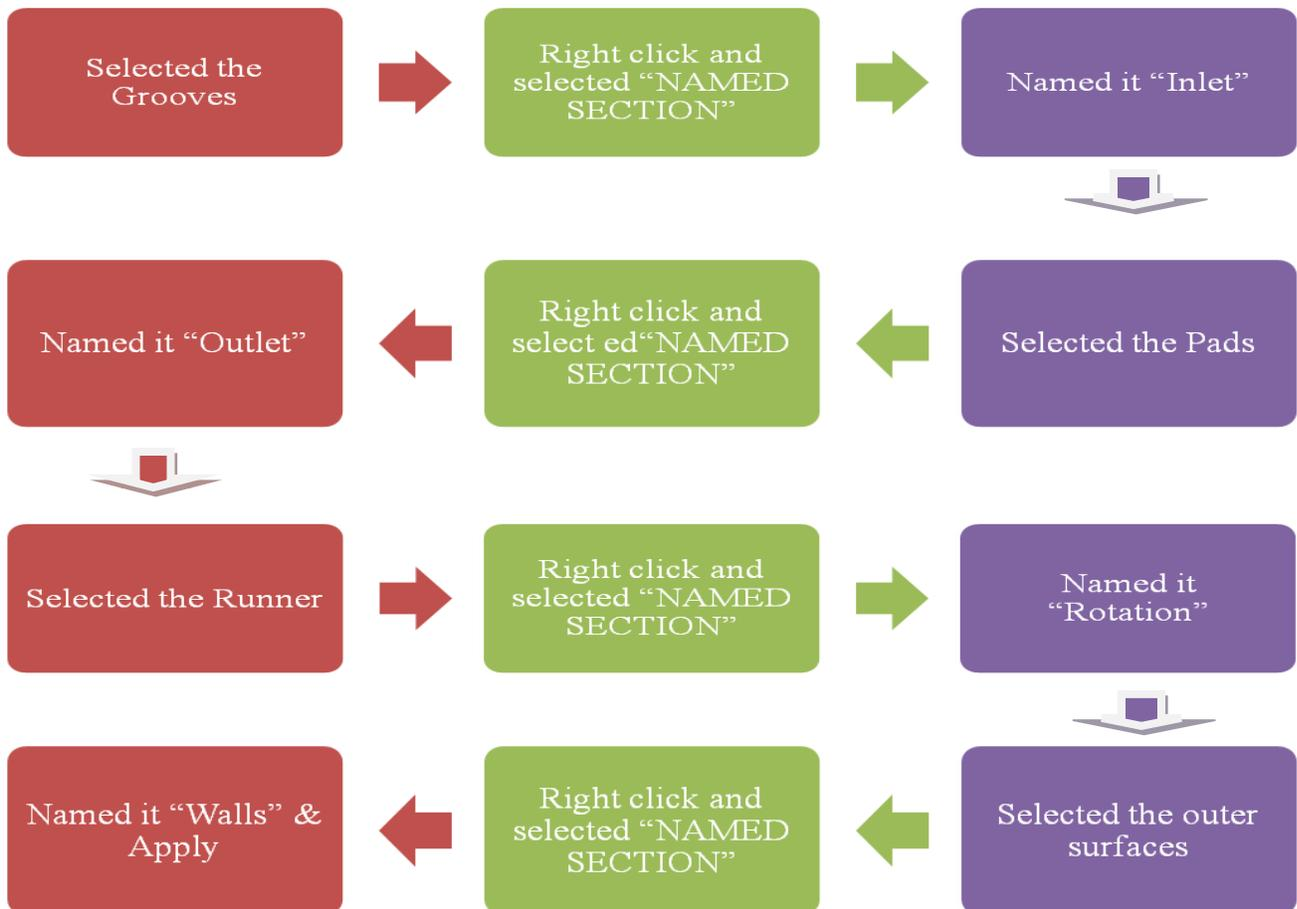
**STEP 2**→Geometry

For the geometry of the surface:-





Now for creation of Named Sections:-



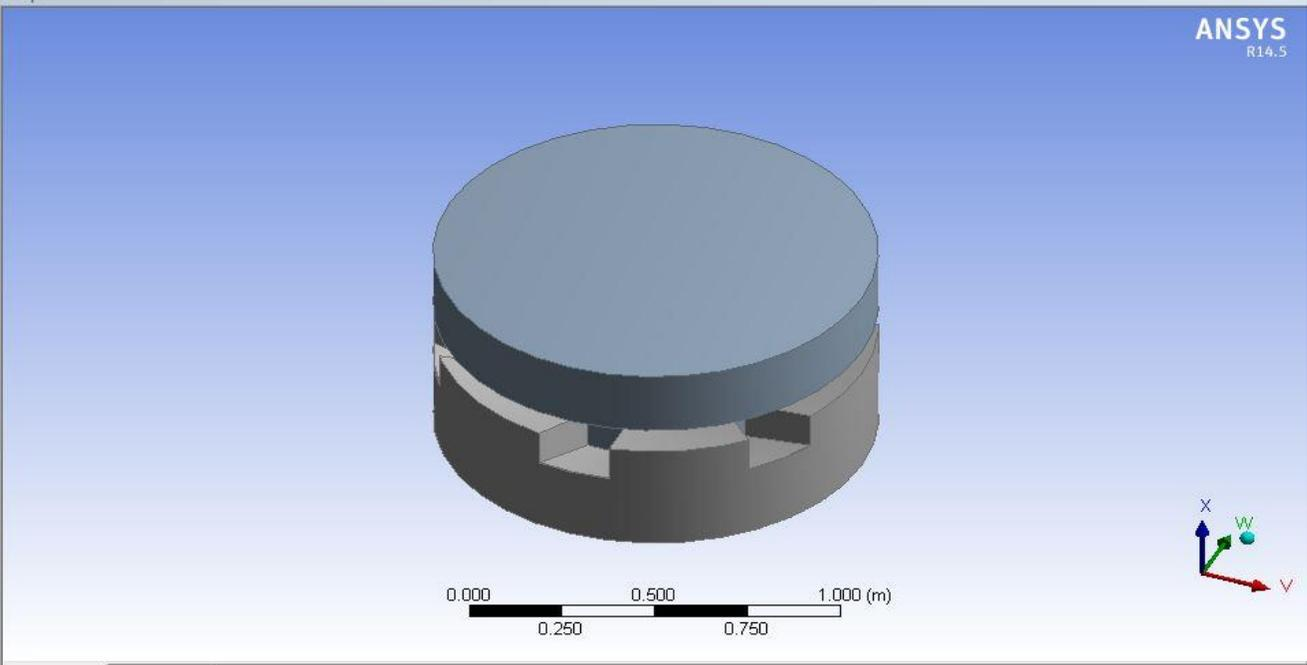


Fig 3.8

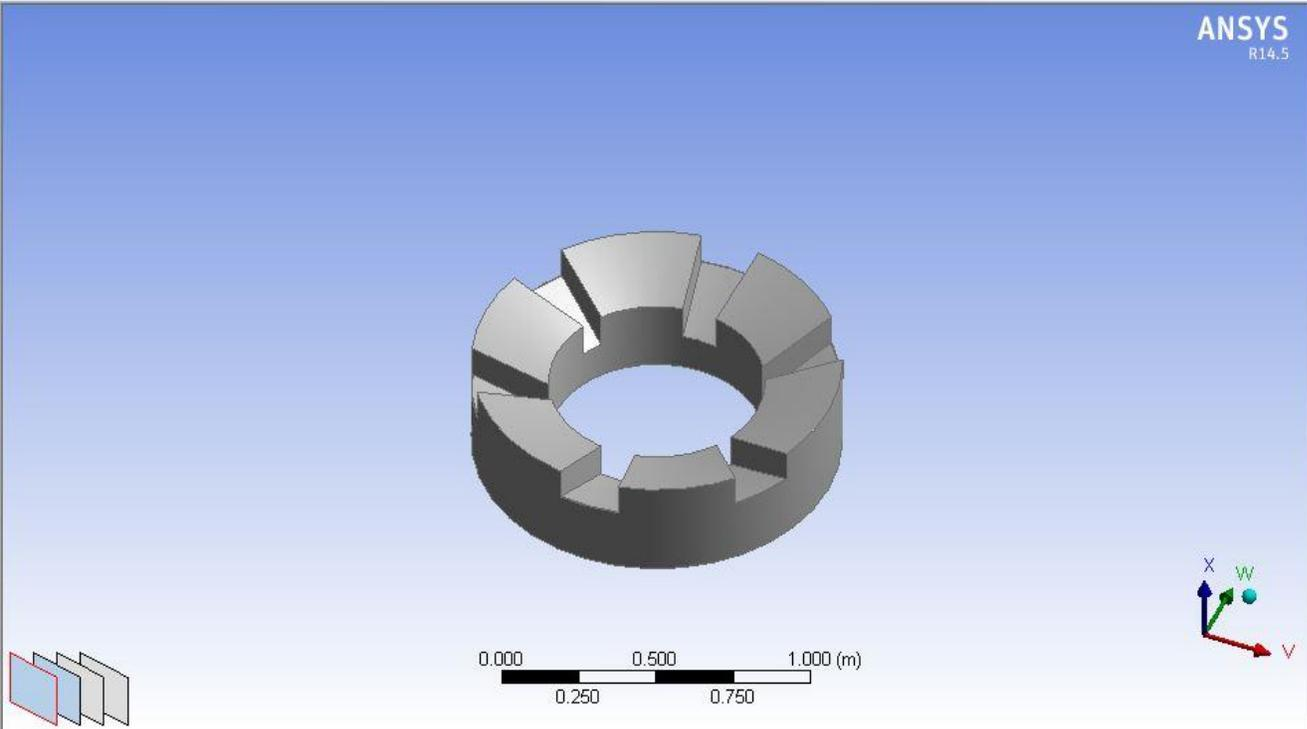


Fig 3.9

**STEP 3:- Mesh**

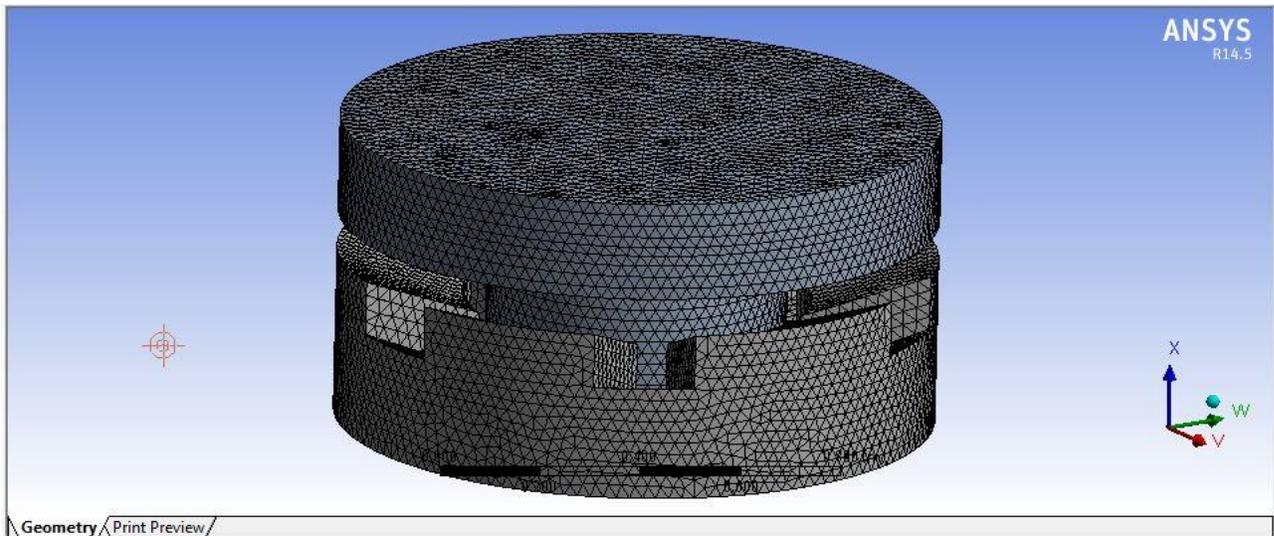


Fig 3.10

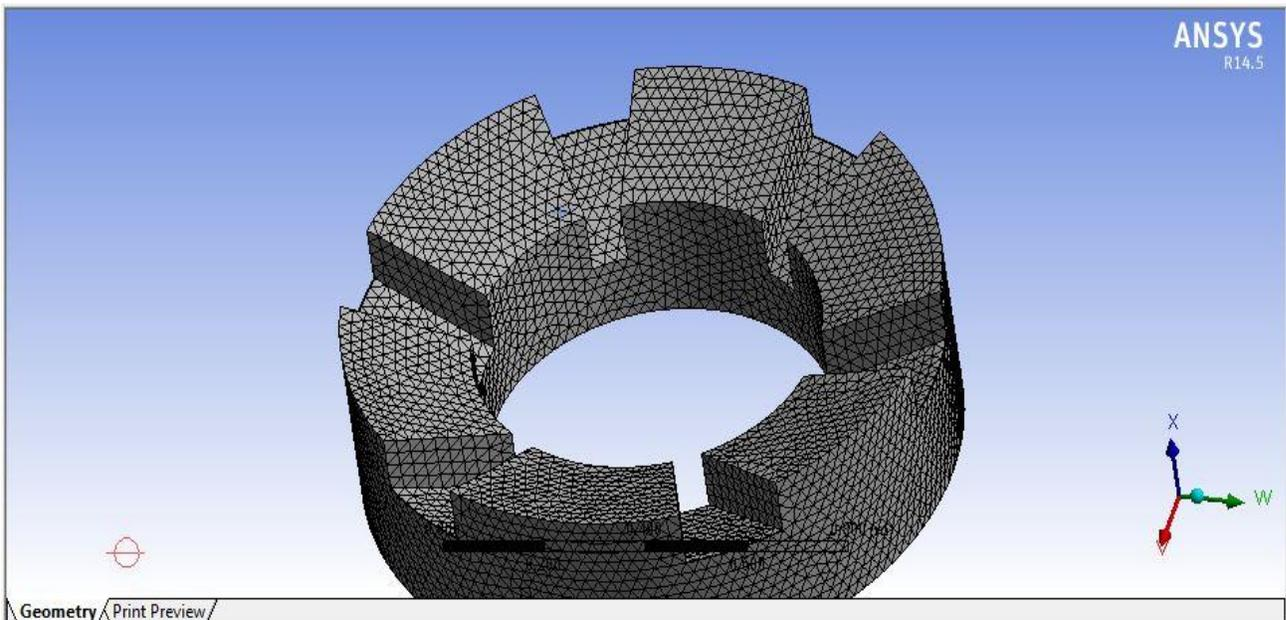
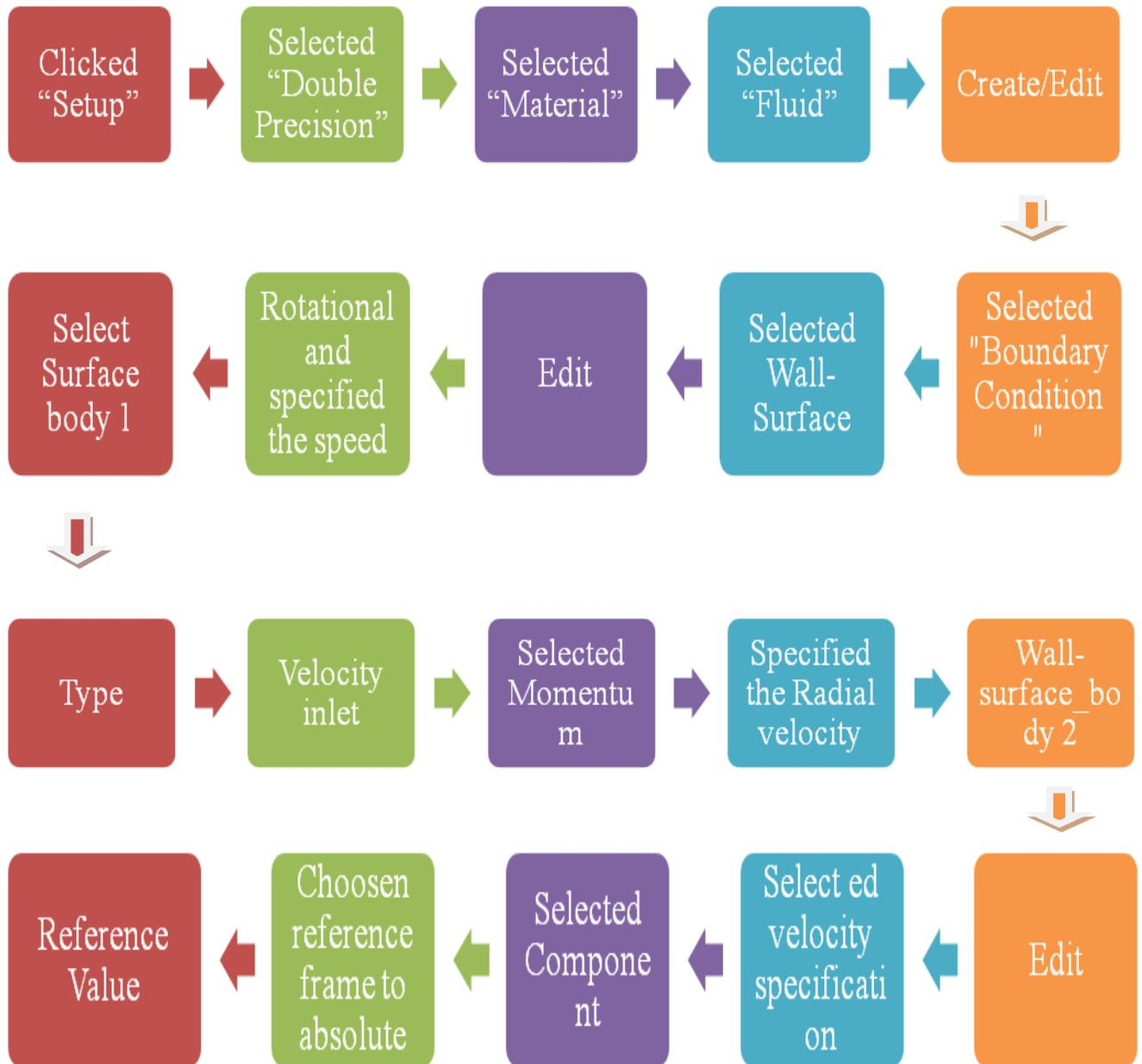
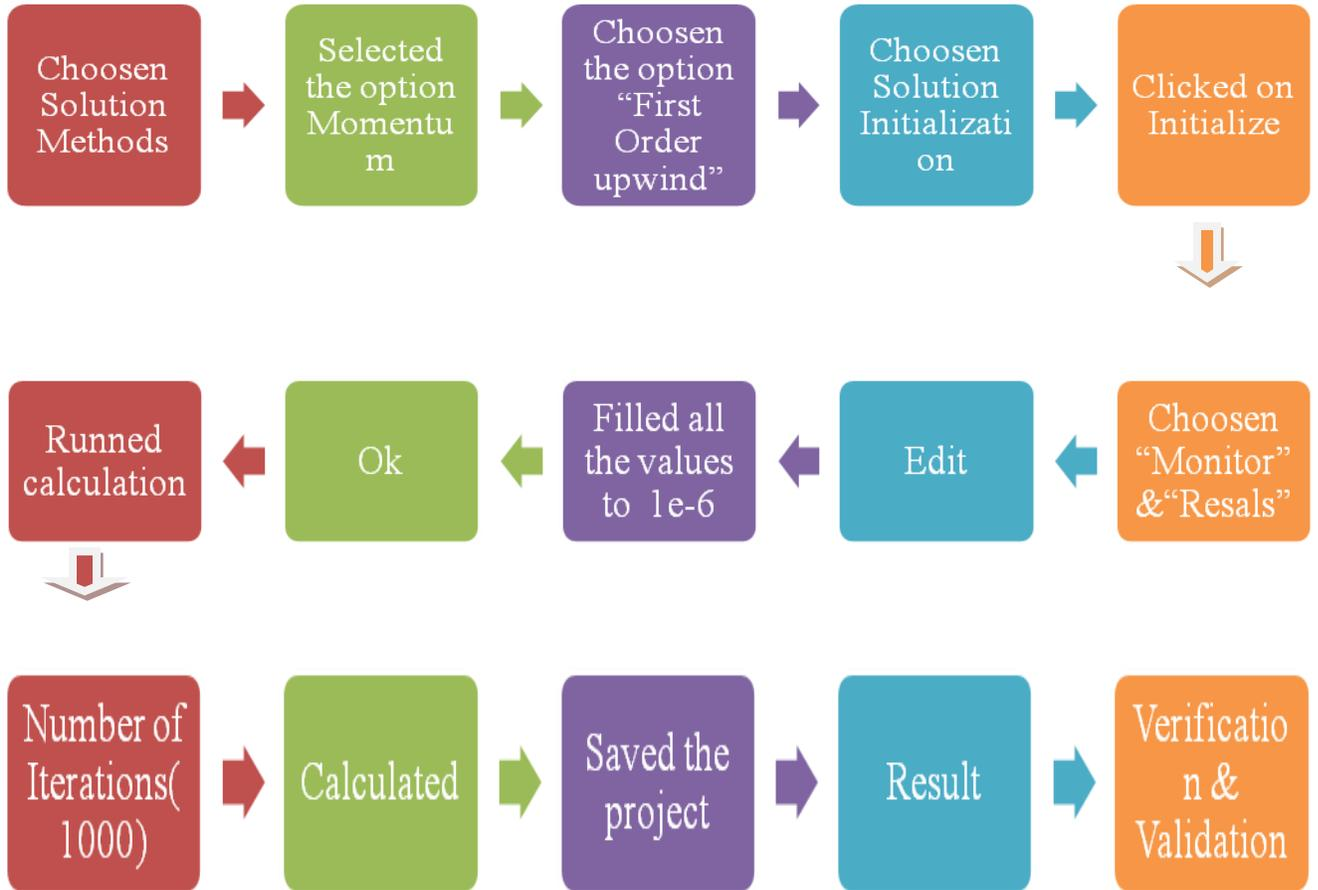


Fig 3.11

**STEP 4:- Setup**



**STEP 5:- Solution**



## Chapter-4

### Results & Discussion

This chapter deals with the results obtained from the computed film thickness and pressure profile under isothermal condition:-

Table 4.1: INPUT DATA

PAPARAMETERS	SYMBOL	VALUE
Pad extent angle in radians $\beta$	$\beta$	$\pi/6$
Pad thickness in m.	$t_p$	0.097
Inner radius of the pad in meter	$R_1$	0.7
Outer radius of the pad in meter	$R_2$	1.2
Nodes in theta direction (tangential direction)	n	10
Nodes in radial direction	m	10
Min. film thickness in meter	$a (=R_2/2.38)$	0.5042
Max. film thickness/min. film thickness	$(a+b)/a$	2.19
Tilt parameter	$\varepsilon (= \gamma R_2 / h_1)$	0.74732
Tilt about pitch line in radians	$\gamma$	2 radians
Dynamic co-efficient of viscosity of SAE 30 lubricant at 50°C $NSm^{-2}$	$\eta$	0.04305
Specific gravity of SAE 30 lubricant at 50°C	S	0.898
Thermal Conductivity of SAE 30 lubricant at 50°C  Using Cragoe's formula: $k = \frac{0.28}{(1 - 0.00054t)} * 10^{-3}$ {in c.g.s. units(t in °C)}	$k_h$	$3.03385 * 10^{-4}$  3.03385 in S.I
Thermal Conductivity of the pad in W/mK	$k_p$	50

The result obtained as a result of FDM analysis using MATLAB software has been plotted and tabulated as below:

Table 4.2: NON-DIMENSIONAL FILM THICKNESS AT DIFFERENT NODAL POINTS

(For 8X8 grid of the pad)

Radius In meter	Angles in radians							
	0	0.0582	0.1745	0.2327	0.2909	0.4072	0.4654	0.5236
0.7000	1.2617	1.2271	1.1912	1.1543	1.1165	1.0780	1.0391	1.0000
0.7714	1.2884	1.2503	1.2107	1.1700	1.1283	1.0860	1.0431	1.0000
0.8429	1.3151	1.2734	1.2302	1.1858	1.1402	1.0939	1.0471	1.0000
0.9143	1.3418	1.2966	1.2498	1.2015	1.1521	1.1019	1.0511	1.0000
0.9857	1.3685	1.3198	1.2693	1.2172	1.1640	1.1098	1.0551	1.0000
1.0571	1.3952	1.3430	1.2888	1.2330	1.1759	1.1178	1.0591	1.0000
1.1286	1.4219	1.3661	1.3083	1.2487	1.1878	1.1258	1.0631	1.0000
1.2000	1.4486	1.3893	1.3278	1.2645	1.1997	1.1337	1.0671	1.0000

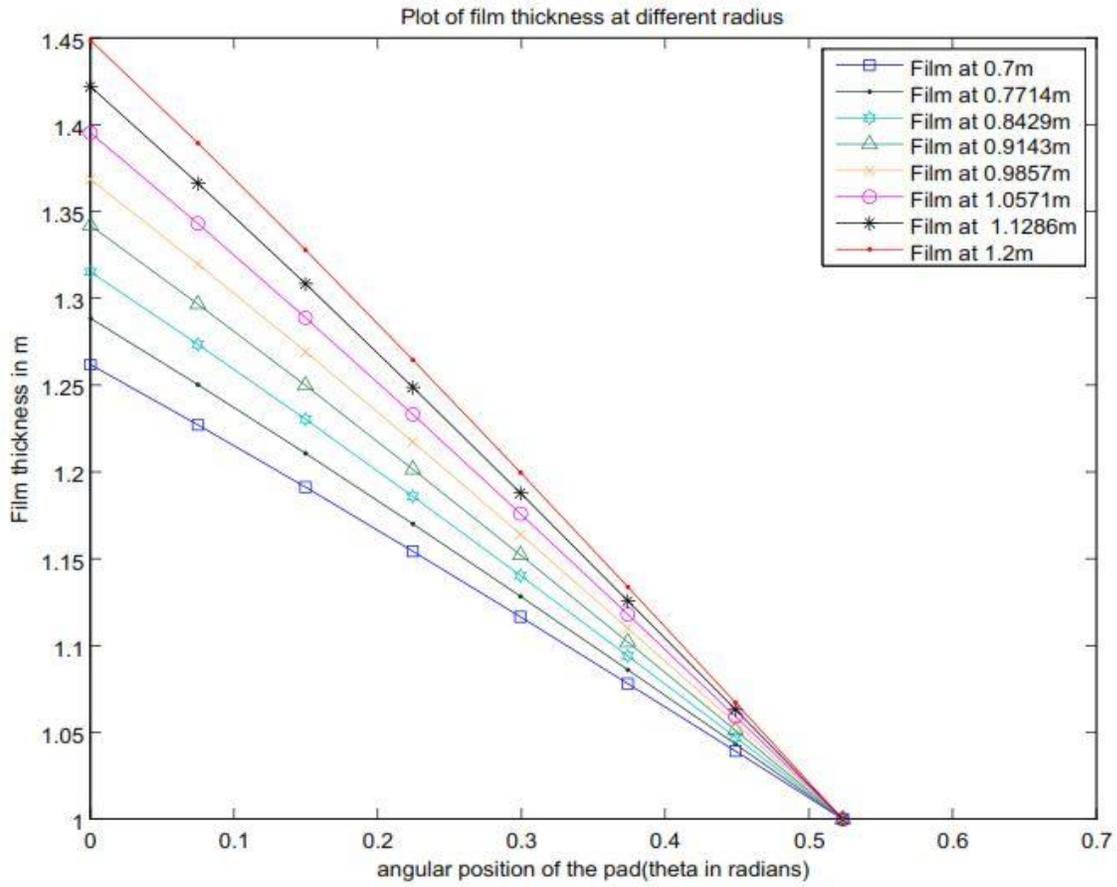
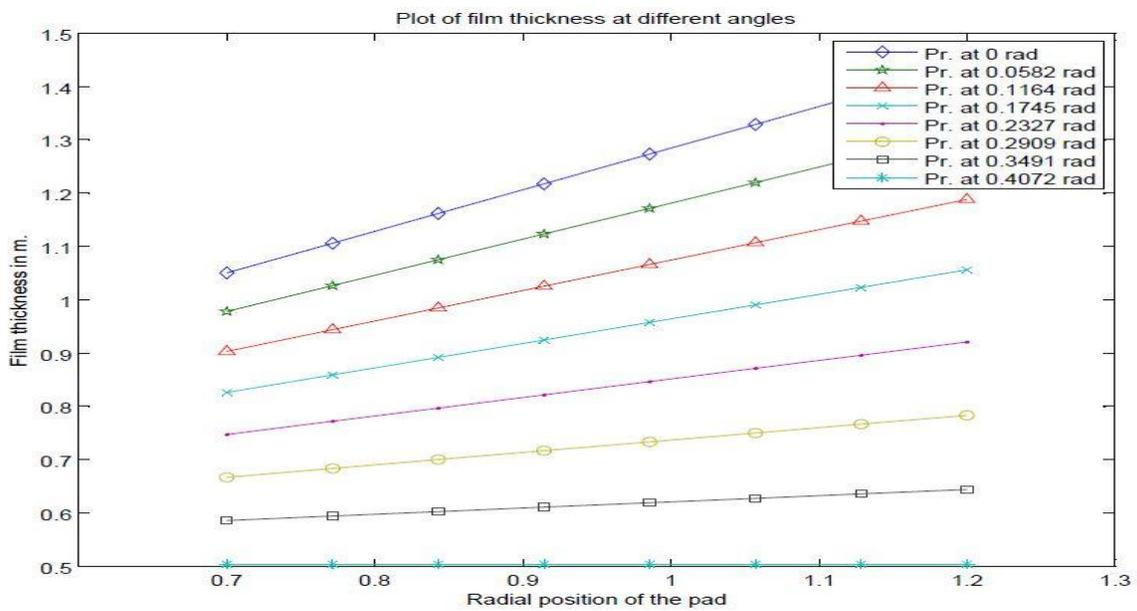


Fig 4.1



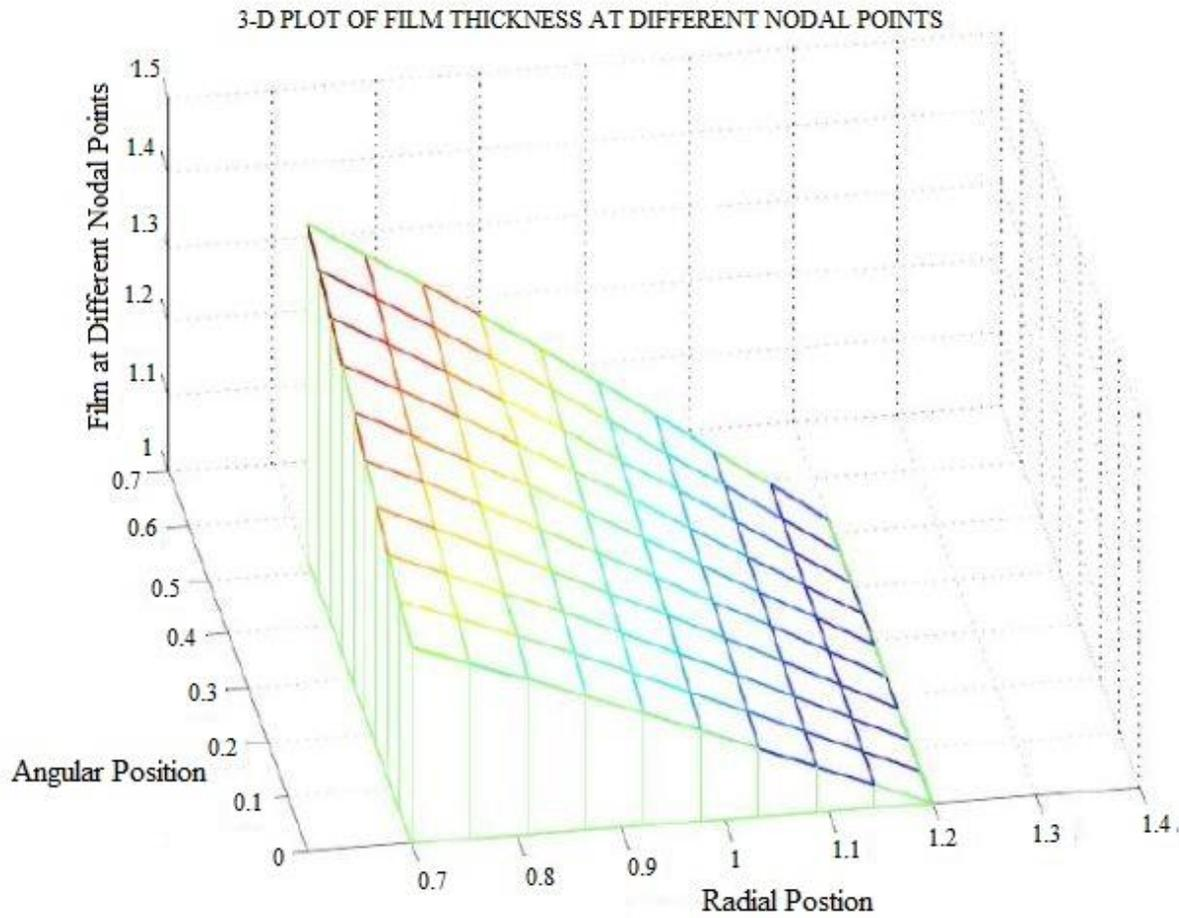


Fig.4.3 Film thickness at different nodal points

Table 4.3: NON-DIMENSIONAL PRESSURE DIST. AT DIFFERENT NODAL POINTS:-  
10<sup>th</sup> iteration result (for 8X8 grid of the pad)

Radius In meter	0	0.0582	0.1745	0.2327	0.2909	0.4072	0.4654	0.5236
0.700	0	0	0	0	0	0	0	0
0.7714	0	0.0786	0.1245	0.1233	0.1165	0.0714	0.0394	0
0.8429	0	0.1404	0.2445	0.2649	0.1945	0.1616	0.0900	0
0.9143	0	0.1507	0.2857	0.2975	0.2495	0.1855	0.1037	0
0.9857	0	0.1527	0.2986	0.3092	0.2958	0.1958	0.1098	0
1.0571	0	0.1430	0.2814	0.2543	0.2857	0.1901	0.1068	0
1.1286	0	0.0861	0.1547	0.1643	0.1562	0.1041	0.0587	0
1.2000	0	0	0	0	0	0	0	0

20<sup>th</sup> iteration result:-

Radius Inmeter	0	0.0582	0.1745	0.2327	0.2909	0.4072	0.4654	0.5236
0.700	0	0	0	0	0	0	0	0
0.7714	0	0.0912	0.1561	0.1590	0.1494	0.0927	0.0510	0
0.8429	0	0.1685	0.3361	0.3458	0.3290	0.2123	0.1167	0
0.9143	0	0.1826	0.3641	0.3849	0.3687	0.2401	0.1327	0
0.9857	0	0.1824	0.3689	0.3922	0.3774	0.2481	0.1375	0
1.0571	0	0.1704	0.3443	0.3666	0.3528	0.2338	0.1300	0
1.1286	0	0.0901	0.1781	0.1867	0.1789	0.1191	0.0669	0
1.2000	0	0	0	0	0	0	0	0

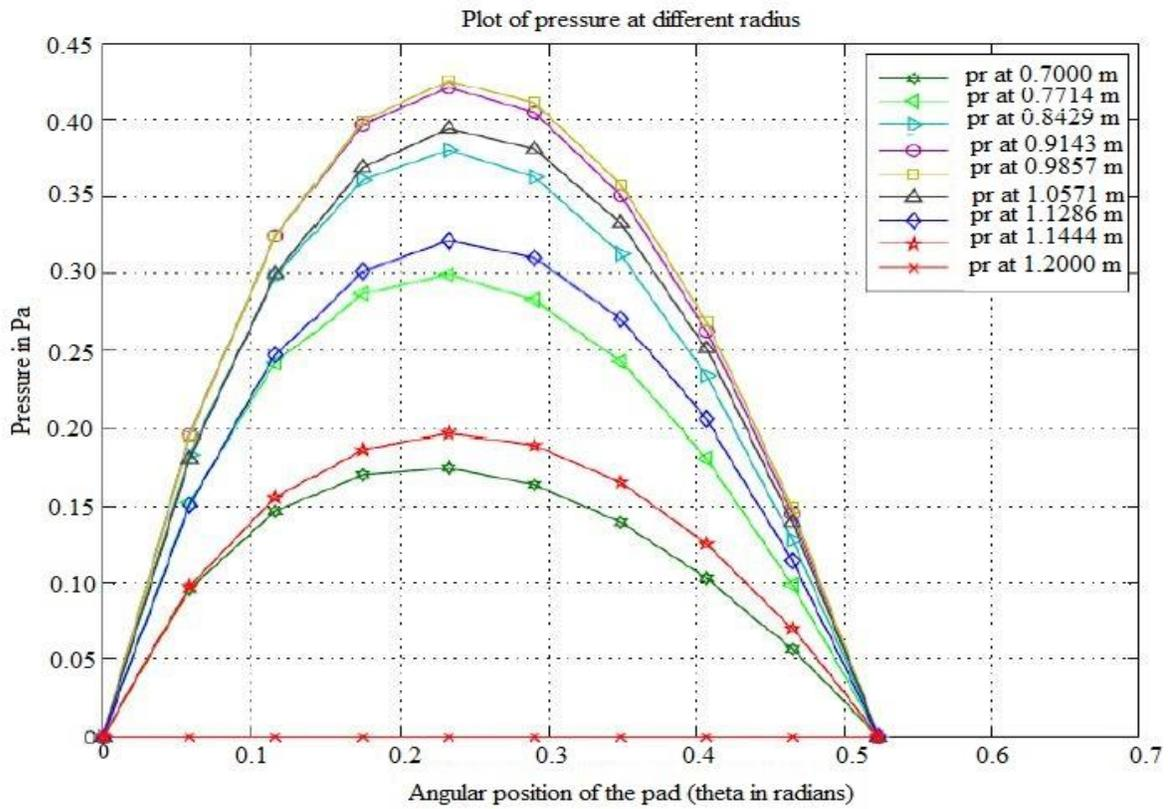


Fig 4.4

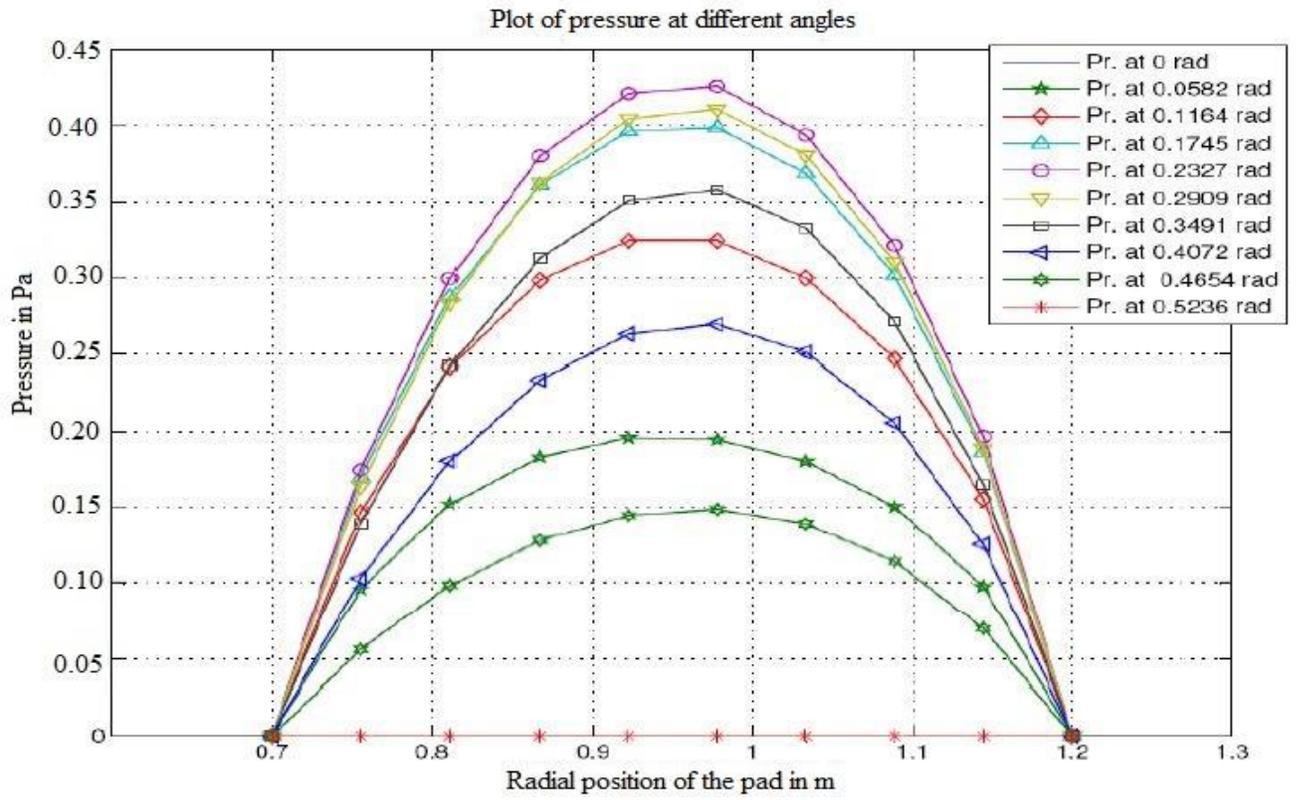


Fig 4.5

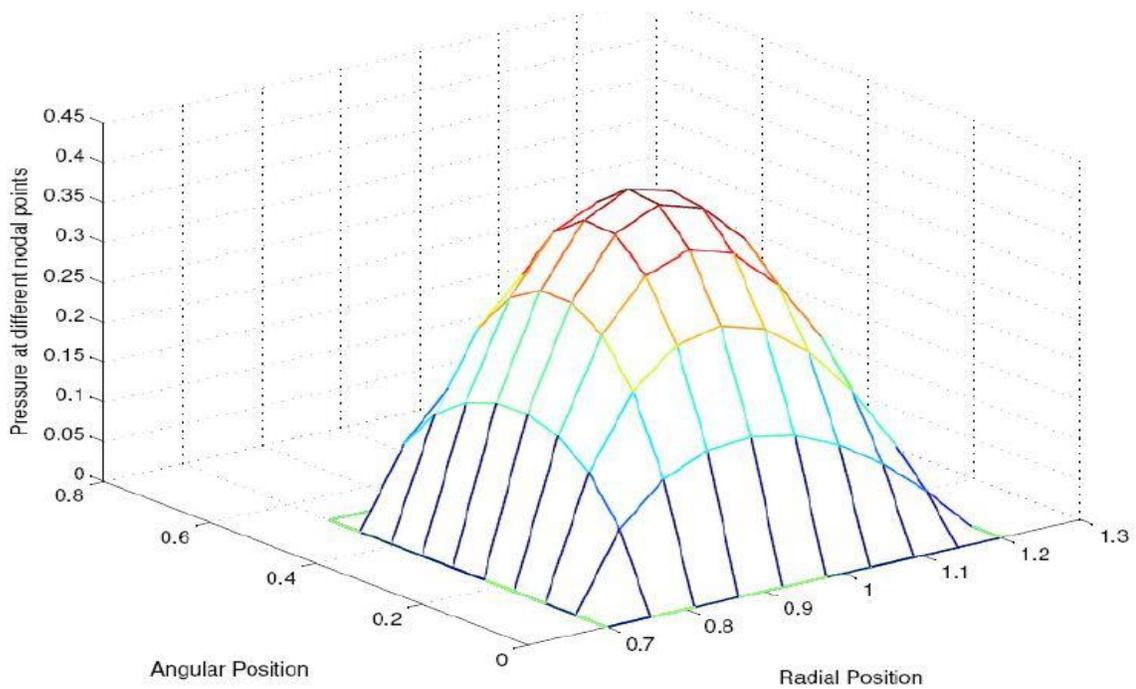


Fig 4.6

**FEM Analysis Result:-** The result obtained as a result of FEM analysis using ANSYS software has been plotted below:

Pressure Contour:-

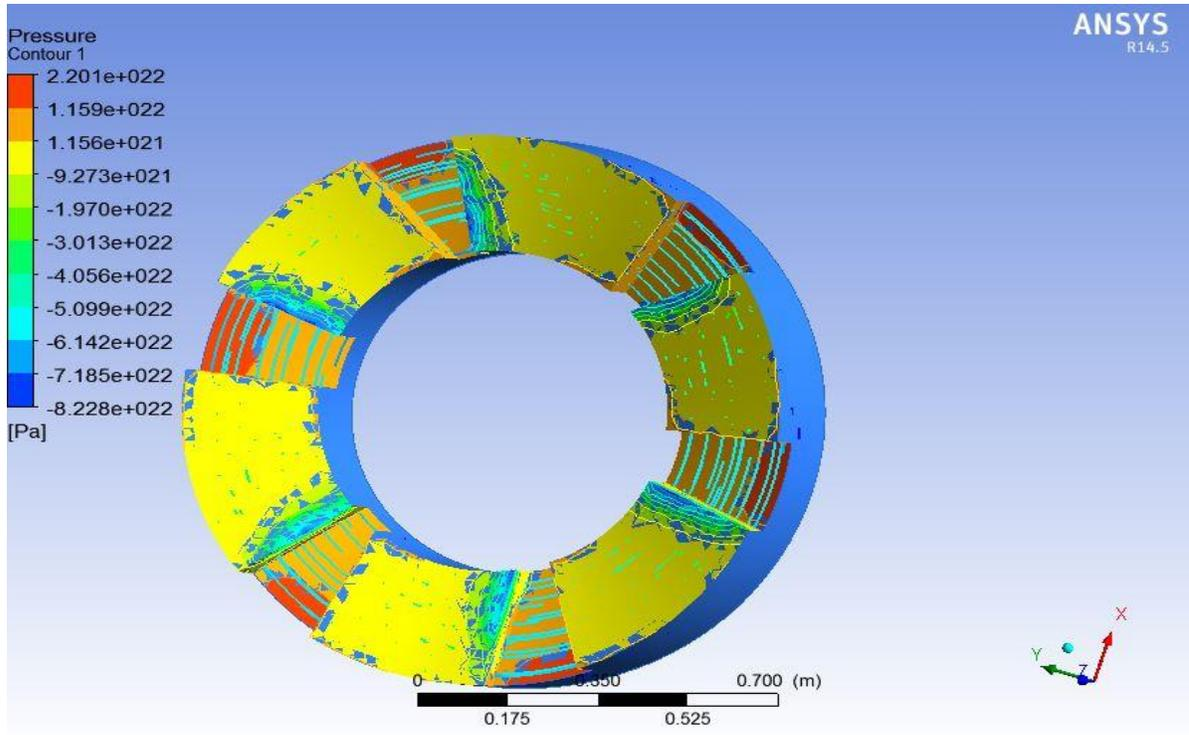


Fig 4.7

Temperature Contour:-

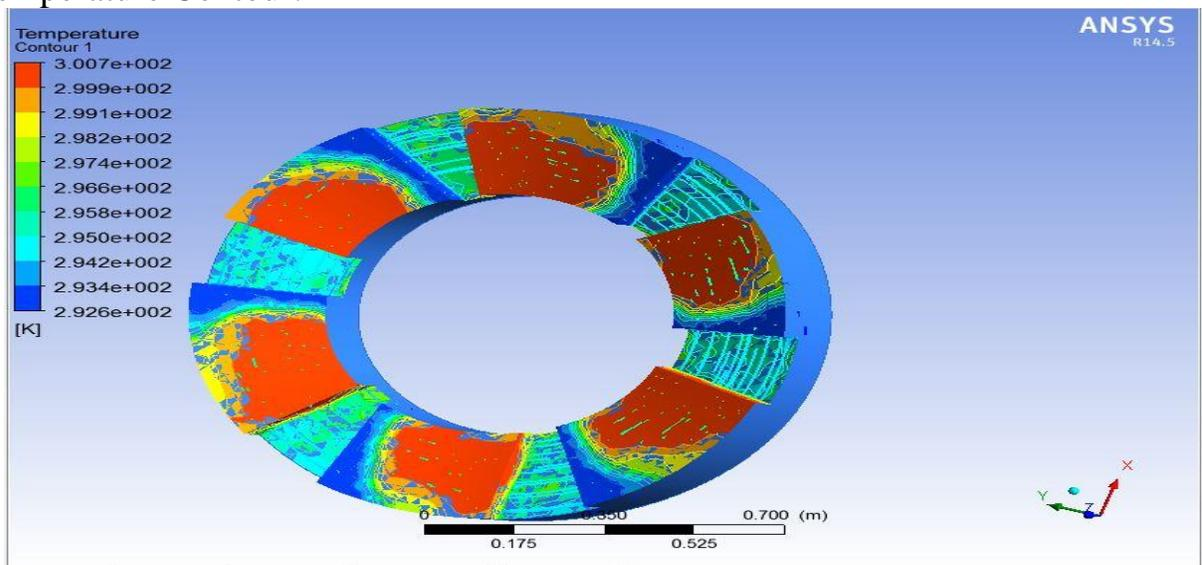


Fig 4.8

Radial Pressure Profile:-

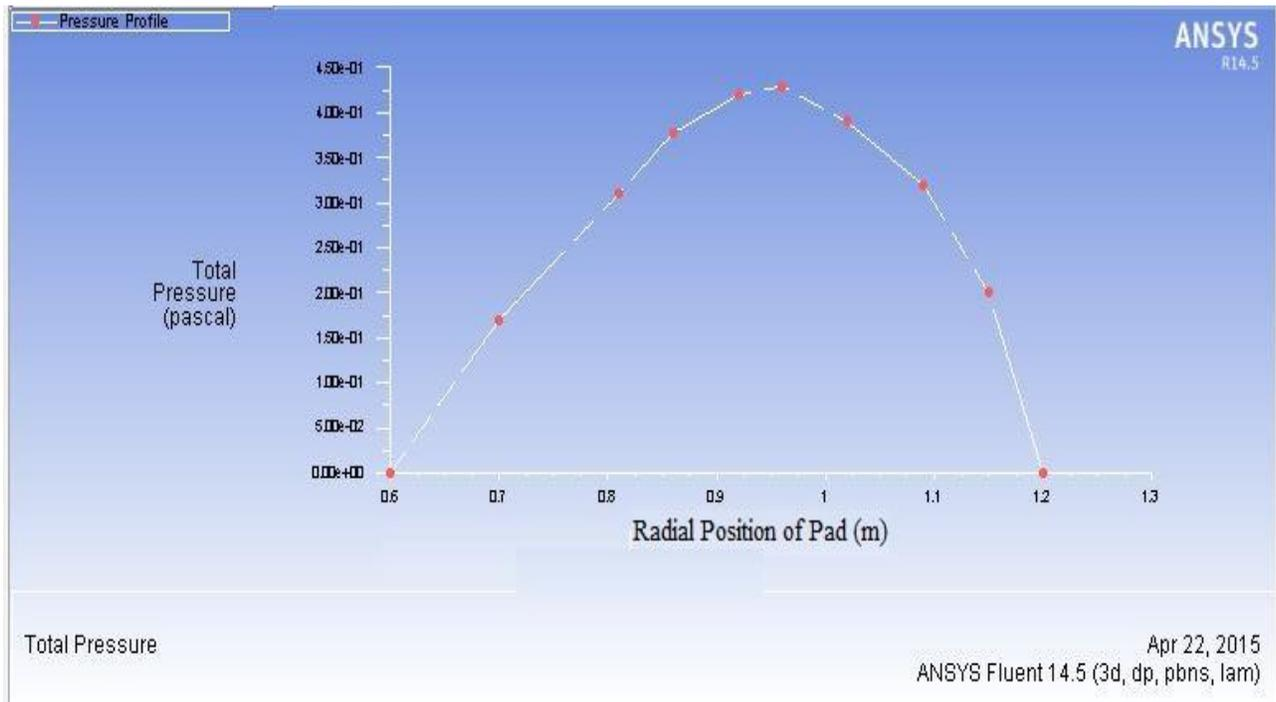


Fig 4.9

Angular Pressure Profile:-

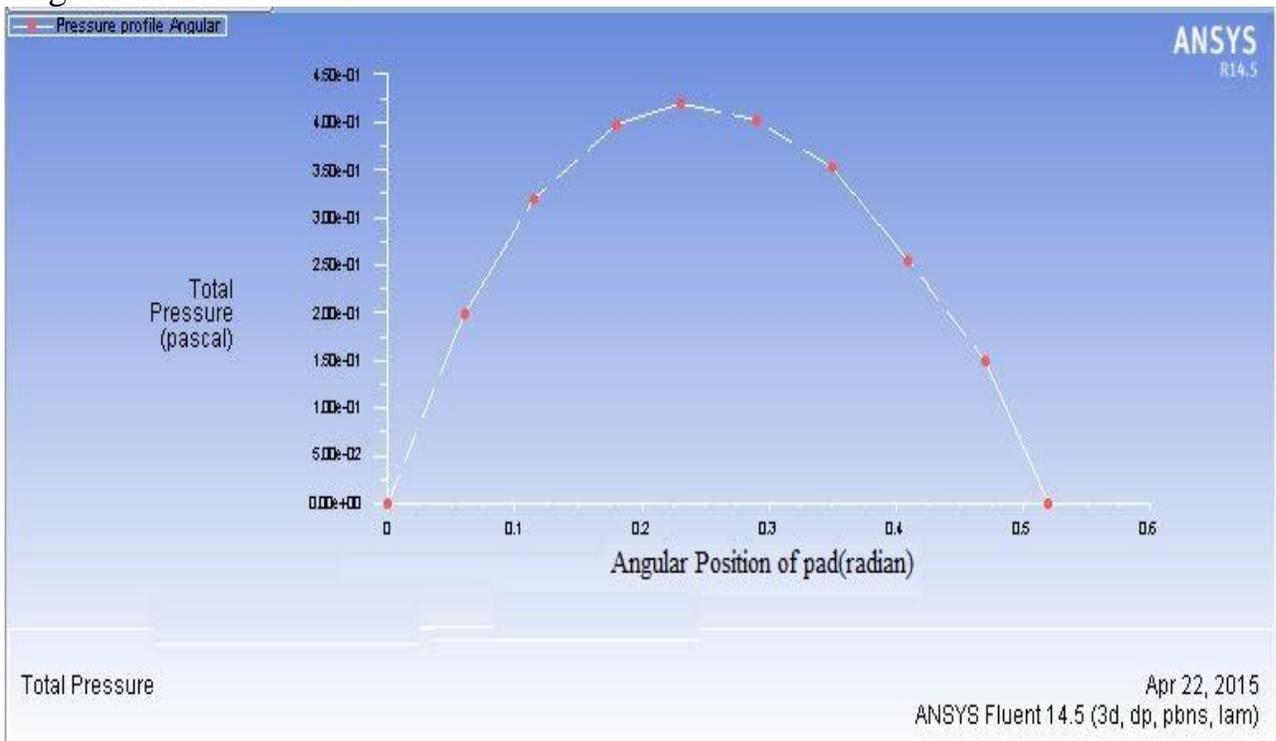


Fig 4.10

Validation of Pressure Profile Obtained By FDM using MATLAB software & FEM Analysis using Ansys software:-

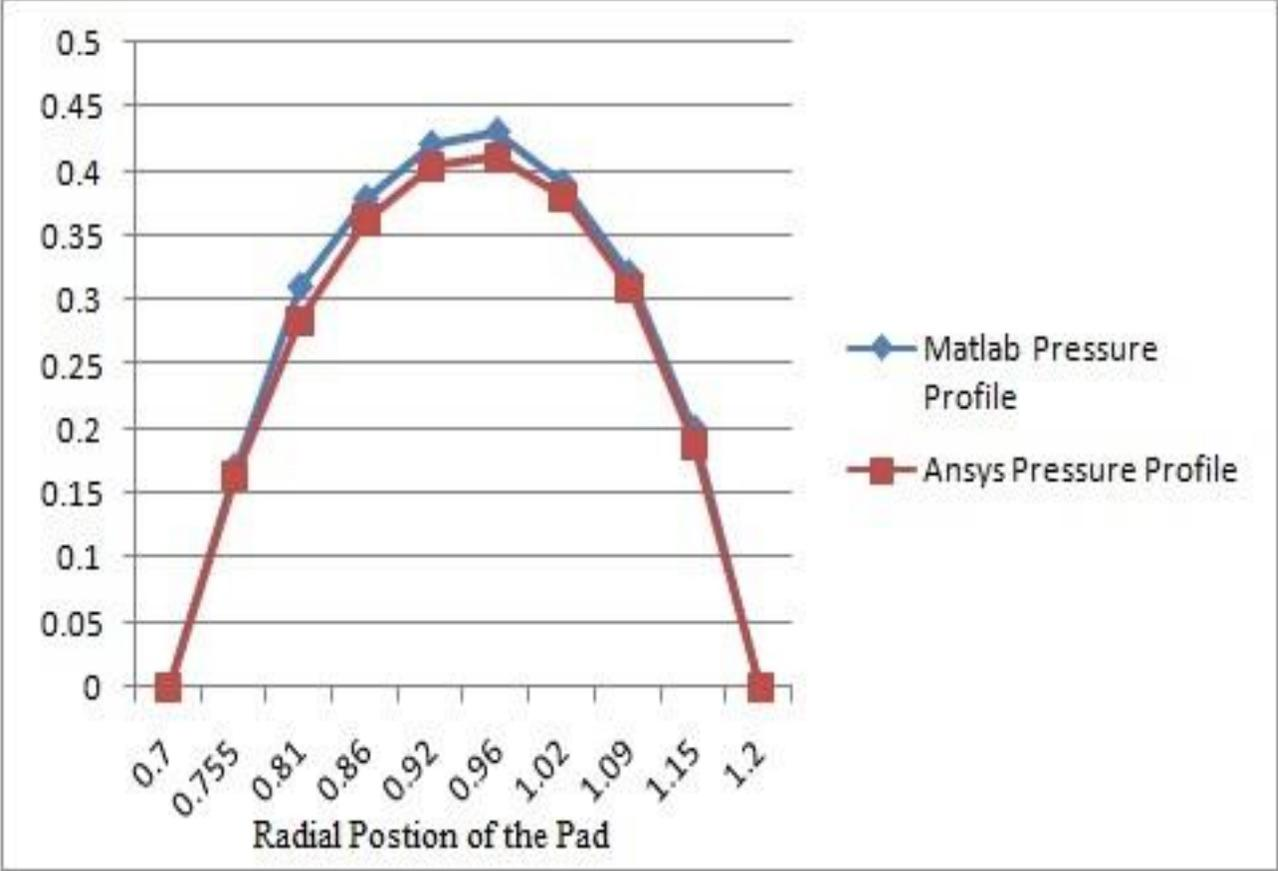


Fig 4.11

## Chapter-6

### Conclusion and Future work

---

#### Conclusions: Isothermal analysis

- Film thickness increases from inner radius to outer radius at a fix angle.
- Both in radial as well as in tangential direction the film thickness varies.
- At a given radius film thickness decreases linearly from maximum to minimum in the direction of rotation.
- The pressure developed along the direction of flow due to the hydrodynamic action is maximum corresponding to the mean radial (0.9857 m.) position.
- The pressure developed across the direction of flow due to the hydrodynamic action is maximum corresponding to the mean angular (0.2327 rad.) position.

#### Future Work:-

- Development of program with thermal effect
- FEM Analysis of Pad thrust bearing and comparing with FDM Analysis result in case when Dynamic Viscosity, Thermal Conductivity are dependent on Temperature.
- Developing empirical relation for film thickness, Temp rise, and Traction Coefficient in case of thermal effect.

## References

---

- [1] Ashour N. M. A. E., Athre K., Nath Y. and Biswas S., 2003 “Distortion analysis of large thrust bearing on elastic support,” *Wear*, **vol. 147**, pp. 421-430
- [2] Ma, C., Zhu, H.: An optimum design model for textured surface with elliptical-shape dimples under hydrodynamic lubrication. *Tribol. Int.* 44, 987–995 (2011)
- [3] Cupillard, S., Glavatskih, S., Cervantes, M.J.: 3D thermohydro- dynamic analysis of a textured slider. *Tribol. Int.* 42, 1487–1495 (2009)
- [4] Ku C-P (2003) Effects of compliance of hydrodynamic thrust bearings in hard disk drives on disk Vibration. *IEEE Trans Mag33*: 2641–2643
- [5] Ighil N. Tala, Maspeyrot P., Fillon M. and Bounif A., 2007 “ Effects of surface texture on journal-bearing characteristics under steady-state operating conditions” *IMEchE Part J*, **vol.221**, pp.623-633
- [6] Hashimoto H., 1990 “Performance Characteristic Analysis of Sector- Shaped Pad Thrust Bearings in Turbulent Inertial Flow Regime Under three types of Lubrication Condition” *Transactions of the ASME*, **vol.112**, pp. 477-485
- [7] Khonsari M. M. and Booser E. R., 2006 “Effect of contamination on the performance of hydrodynamic bearings” *IMEchE Part J*, **vol.220**, pp.419-428
- [8] Ighil N. Tala, Maspeyrot P., Fillon M. and Bounif A., 2007 “ Effects of surface texture on journal-bearing characteristics under steady-state operating conditions” *IMEchE Part J*, **vol.221**, pp.623-633
- [9] Storteig E. and White Maurice F., 2009 “Dynamic characteristics of hydrodynamically lubricated fixed-pad thrust bearings”, *Wear*, **vol.232**, pp. 250-255
- [10] Stahl J. and Jacobson B. O., 2001 “Design functions for hydrodynamic bearings”, *IMEchE Part J*, **vol.215**, pp.405-415
- [11] Sharma R. K., and Pandey R. K., 2008 “Thermohydrodynamic analysis of infinitely wide cycloidal profiled pad thrust bearing with rough surface and a comparison to plane profiled pad” *Lubrication Science*, **vol.20**, pp. 183-203
- [12] Glavatskikh Sergei B., 2001 “Steady State Performance Characteristics of a Tilting Pad Thrust Bearing”, *Transactions of the ASME*, **vol.123**, pp. 608-615

- [13] Stahl J. and Jacobson B. O., 2001 “Design functions for hydrodynamic bearings”, *IMechE Part J*, **vol.215**, pp.405-415
- [14] Glavatskih S. B., Fillon M. and Larsson R., 2002 “The Significance of Oil Thermal Properties on the Performance of a Tilting-Pad Thrust Bearing”, *Transactions of the ASME*, **vol.124**, pp. 377-385
- [15] Markin D., McCarthy D. M. C. and Glavatskih S. B., 2003 “A FEM approach to simulation of tilting-pad thrust bearing assemblies”, *Tribology International*, **vol.36**, pp. 807-814
- [16] Glavatskih S. B., 2003 “Evaluating Thermal Performance of a PTFE-Faced Tilting Pad Thrust Bearing”, *Transactions of the ASME*, **vol.125**, pp.319-324
- [17] Wasilczuk M., 2003 “Comparison of an Optimum-Profile Hydrodynamic Thrust Bearing with a Typical Tilting- Pad Thrust Bearing”, *Lubrication Science*, **vol.15**, pp. 265-273
- [18] Yuan X., Zhu J., Chen Z., Wang H. and Zhang C., 2003 “A Three-Dimensional TEHD Model and an Optimum Surface Profile Design of Pivoted Pad Thrust Bearings with Large Dimensions”, *Tribology Transactions*, **vol.46**, pp. 153-160
- [19] Jang G. H., Kim K. S., Lee H. S., and Kim C. S., 2004 “Analysis of a Hydrodynamic Bearing of a HDD Spindle Motor at Elevated Temperature”, *Transactions of the ASME*, **vol.126**, pp. 353-359 43
- [20] Bryant M D and Lee S., 2004 “Resistive field bond graph models for hydrodynamically lubricated bearings”, *IMechE*, **vol.218**, pp. 645-654
- [21] Glavatskih S. B., 2004 “A method of temperature monitoring in fluid film bearings”, *Tribology International* , **vol.37**, pp.143-148
- [22] Glavatskih S. B., and DeCamillo S., 2004 “Influence of oil viscosity grade on thrust pad bearing operation”, *IMechE Part J*, **vol.218**, pp.401-412
- [23] Glavatskih S. B., McCarthy D. M. C. and Sherrington I., 2005 “Hydrodynamic Performance of a Thrust Bearing with Micropatterned Pads”, *Tribology Transactions*, **vol.48**, pp. 492-498
- [24] Kim D., Jackson R. L. and Green I., 2006 “Experimental Investigation of Thermal and Hydrodynamic Effects on Radially Grooved Thrust Washer Bearings”, *Tribology Transactions*, **vol.49**, pp. 192-201

- [25] Yang S. H., Kim C. and Lee Y. B., 2006 “Experimental study on the characteristics of pad fluttering in a tilting pad journal bearing” *Tribology International*, **vol.39**, pp.686-694
- [26] Bouyahia F., Hajjam M., Khlifi M El, and Souchet D., 2006 “Threedimensional non-Newtonian lubricants flows in sector-shaped, tilting-pads thrust bearings” *IMechE Part J*, **vol.220**, pp.375-384
- [27] Glavatskih S. B. and Fillon Michel, 2006 “TEHD Analysis of Thrust Bearings With PTFE-Faced Pads”, *Transactions of the ASME*, **vol.128**, pp. 49-58
- [28] Khonsari M. M. and Booser E. R., 2006 “Effect of contamination on the performance of hydrodynamic bearings” *IMechE Part J*, **vol.220**, pp.419-428